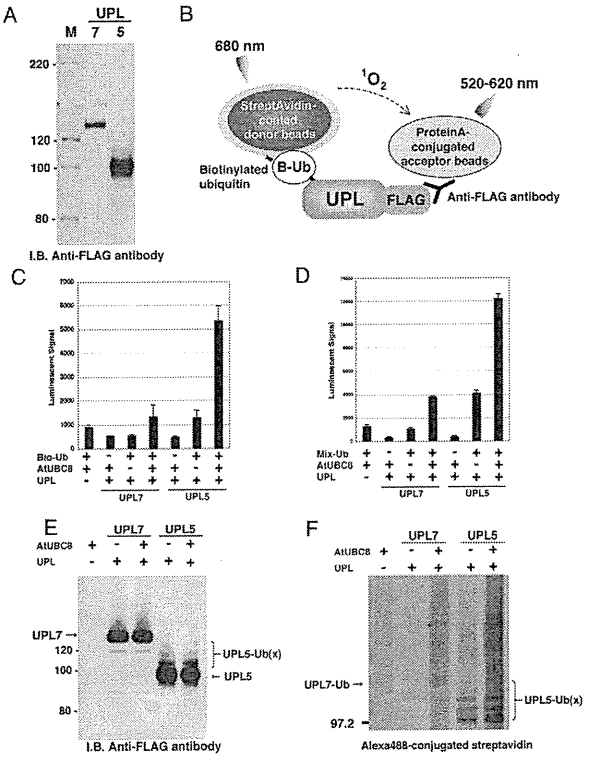

Figure 2

Analysis of recombinant Arabidopsis HECT-type E3 ligases (UPL7 and UPL5). A, Production of FLAG-tagged recombinant UPL proteins was detected by immunoblot analysis. For analysis, 5 μl of crude recombinant UPL proteins were loaded, and detected by immunoblot analysis using anti-FLAG antibody. B, Schematic diagram of detection of ubiquitin-conjugation of UPLs by luminescent analysis. Protein A-conjugated acceptor beads and streptavidin-coated donor beads were bound to anti-FLAG antibody bound to FLAG-tagged recombinant UPLs and biotinylated ubiquitin, respectively, and detected by same principle and procedure described in Figure 1B. C, The ubiquitination of crude recombinant UPL7 and UPL5 was detected by luminescent analysis described in B. Bio-Ub means biotinylated ubiquitin. D, polyubiquitination of crude recombinant UPL7 and UPL5 was detected by luminescent analysis with anti-His antibody. Mix-Ub indicated the mixture of His-tagged and biotinylated ubiquitin. E and F, Mobility shift of UPLs (E) and formation of polyubiquitin chains (F) were detected by immunoblot using anti-FLAG antibody and Alexa488-conjugated streptavidin, respectively. The polyubiquitination reaction was done with FLAG-tagged recombinant UPLs in presence or absence of crude AtUBC8, and then recombinant UPLs were purified by anti-FLAG antibody-conjugated agarose. Error bars represent standard deviations from three independent experiments.

and biotinylated ubiquitin were used. When biotinylated ubiquitin is conjugated to the UPL-FLAG, a high luminescent signal is obtained (Fig. 2B). As a result of the analysis, ubiquitin-conjugation of UPL5 was observed (Fig. 2C). In addition, polyubiquitin chains formed by UPLs were detected with the luminescence assay using His-tagged and biotinylated ubiquitin. To subtract polyubiquitin chain formation from endogenous E2 and E3 in wheat cell-free system, the assay was performed without recombinant UPL and only low signal was detected (Fig. 2D, "UPL-" lane). As expected, luminescent signal was observed in recombinant UPL5 and UPL7 (Fig. 2D). Although the luminescent signal of UPL7 was lower than that of UPL5, the signal was still two-fold higher than the endogenous background signal. These results were confirmed by immunoblot analysis that showed distinct mobility shifts of UPL5 (Fig. 2E) when detecting FLAG-tagged UPLs, and polyubiquitin chain formation of UPL5 monitoring Alexa488-conjugated streptavidin (Fig. 2F). Comparing the amount of polyubiquitin chain formation in absence of UPLs (Fig. 2F, "UPL-" lane), UPL7 formed weak but distinct polyubiquitin chains in presence of AtUBC8. These luminescent signals were consistent with immunoblot data. Interestingly, polyubiquitin chains were formed by UPL5 without supplementing exogenous E2 protein (Fig. 2D and 2F, "AtUBC8-" lane), suggesting that wheat germ extract has endogenous E2 activity as well as endogenous E1 activity. These data indicate that the wheat cell-free production system is able to produce high molecular weight proteins in functional forms and that our luminescence method can detect activity of HECT-type E3 ligases without purification. This is the first data showing that full length recombinant HECT-type E3s have ubiquitin-conjugating and polyubiquitination activity. Taken together, the luminescent method based on the wheat cell-free system could be useful for biochemical analysis of HECT-type E3 ligases.

Detection of Polyubiquitin Chains by RING-Type CIP8 E3 Ligase

It is reported that at least 469 predicted RING-type E3 ligases are encoded in the Arabidopsis genome [25]. Like the HECT-type E3, we attempted to express and carry out the functional analysis of the RING-type E3 ligases. In this study, we selected CIP8 as a model RING-type E3 ligase, which is reported to possess a RING finger motif and have typical features of an E3 ligase [26]. At first, polyubiquitination activity of purified CIP8 in presence or absence of exogenous E1 and purified E2 (AtUBC8) was investigated by luminescence. As shown in Fig 3A, luminescence analysis using His-tagged and biotinylated ubiquitin showed the polyubiquitination of purified CIP8 only when exogenous E1 and purified E2 were added to the reaction mixture. The CIP8-dependent polyubiquitination was

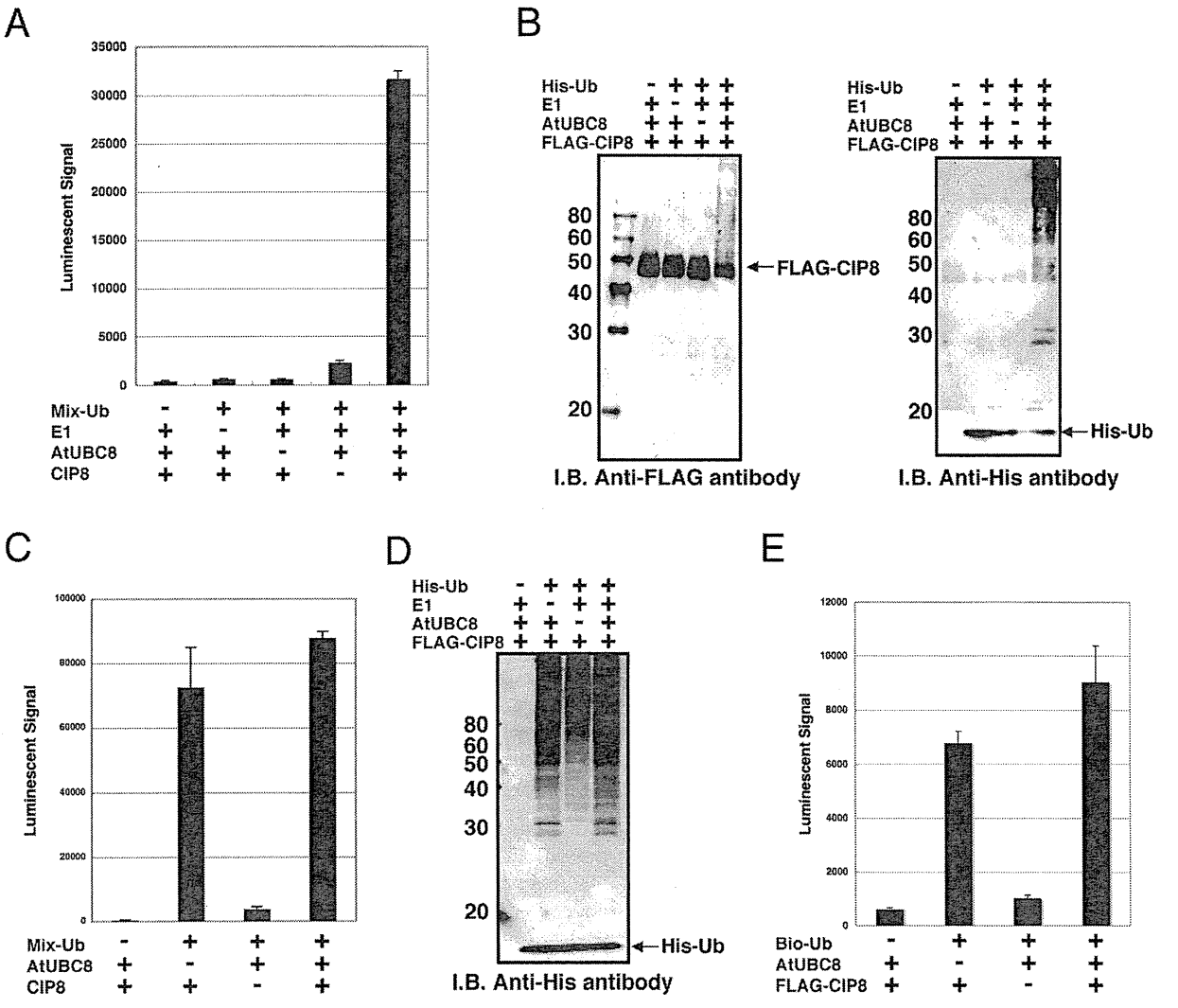

Figure 3

Detection of polyubiquitination and self-ubiquitination of CIP8. A to D, The polyubiquitination assay was carried out with purified (A and B) or crude recombinant CIP8 (C and D) and detected by luminescent analysis with anti-FLAG antibody (A and C) and immunoblot analysis (B and D). His-Ub or Mix-Ub indicate His-tagged ubiquitin or the mixture of FLAG-tagged and biotinylated ubiquitin, respectively. The polyubiquitination assay using luminescent analysis was carried out with recombinant CIP8 without tag in the presence or absence of ubiquitin related components indicated below each graph. E, Ubiquitination of crude recombinant CIP8 was observed by luminescent analysis with anti-FLAG antibody. The assay was carried out with or without biotinylated ubiquitin and crude AtUBC8 recombinant protein. Bio-Ub means biotinylated ubiquitin. Error bars represent standard deviations from three independent experiments.

confirmed by immunoblot analyses detecting both FLAG-CIP8 and His-tagged ubiquitin (Fig. 3B). On the other hand, luminescent analysis with crude CIP8 protein showed high polyubiquitination activity both in the presence or absence of purified E2 (Fig. 3C), and was confirmed by immunoblot analysis with crude protein (Fig. 3D). These data indicated that, like recombinant UPL5, crude CIP8 also utilized endogenous wheat extract E1 and E2 proteins, and therefore we could carry out the simple polyubiquitination analysis of E3 without addition of exogenous E1 and E2 proteins. Furthermore, immunoblot analysis detecting purified CIP8 (Fig. 3B) showed a mobility shift of FLAG-tagged CIP8 to higher molecular weights due to ubiquitination, whereas the mobility of the E2 was

not altered (data not shown). This result indicates that the CIP8-dependent polyubiquitin chains might be elongated on CIP8 itself. This data is consistent with a recent report showing that TRIM5a, a typical RING-type E3 ligase in human, also undergoes self-ubiquitination, forming polyubiquitin chains on itself [27]. To clarify whether the mobility shift of CIP8 was concomitant with polyubiquitin chain formation resulting from self-ubiquitination, we tried to detect ubiquitination of CIP8 by the luminescent method using crude FLAG-CIP8 protein and biotinylated ubiquitin. The luminescent method clearly detected the binding of biotinylated ubiquitin to FLAG-tagged CIP8 both in the presence and absence of exogenous E2 (Fig. 3E). Similar to polyubiquitin formation, the ubiquitination of CIP8 also occurred without the addition of exogenous E2 protein (Fig. 3E, "AtUBC8-" lane). Taken together, these data demonstrate that the luminescent method could detect formation of RING-type CIP8-dependent polyubiquitin chains and self-ubiquitination of crude CIP8.

Screening of RING-Type E3 Ligases Having Polyubiquitination Activity

Recent papers have reported that the polyubiquitin chain is an important biological regulator. Identification of activity and features of E3 ligases offers important information about the ubiquitin-dependent regulation system. Our luminescent method based on the wheat cell-free system produced a simple and high-sensitivity detection of CIP8-dependent polyubiquitin chains without any purification (Fig. 3C). Using these tools, we screened new E3 ligases for the ability to form polyubiquitin chains like CIP8.

The RING-type E3 ligases in Arabidopsis were divided into 30 subgroups based on domain structure, and CIP8 is categorized into subgroup 6 as it contains a coiled-coil domain [25]. Eight other RING-type E3s from subgroup 6 were selected for screening, and the simple polyubiquitination assay was carried out with FLAG-tagged and biotinylated ubiquitins, and the crude recombinant RING-type E3s without addition of exogenous E1 and E2. The screening result showed significant polyubiquitination activity of At1g55530, whereas other RING-E3 proteins were not active (Fig. 4A). Immunoblot analysis of purified recombinant At1g55530 confirmed the polyubiquitination activity and indicated that At1g55530 was self-ubiquitinated (Fig. 4B). The polyubiquitination activity of At1g55530 suggests that it may have a biological role for proteasome-mediated degradation like CIP8 [26]. These results show that the wheat cell-free protein expression system and the luminescent ubiquitination detection method could support functional high-throughput screening of E3 proteins.

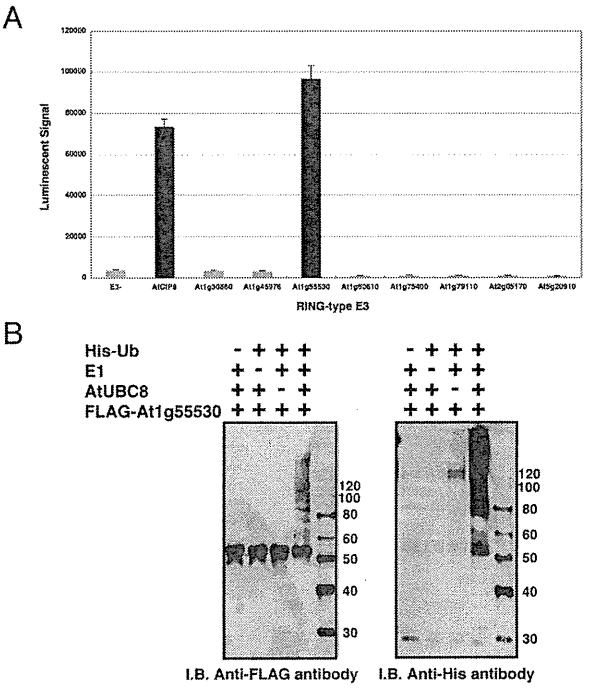

Figure 4
Screening of RING-type E3 ligases having polyubiquitination activity. A, Polyubiquitination reaction of crude recombinant E3 proteins was carried out with mixture of FLAG-tagged and biotinylated ubiquitins, and investigated by luminescent analysis with anti-FLAG antibody. B, Polyubiquitination activity of At1g55530 was confirmed by immunoblot analysis. The assay was carried out using purified recombinant AtUBC8 and At1g55530, and mobility shift of FLAG-tagged At1g55530 and polymer of His-ubiquitin were detected by immunoblot analysis using anti-FLAG and anti-His antibodies, respectively. Error bars represent standard deviations from three independent experiments.

Analysis of the Wheat Cell-free Based Ubiquitination in the Presence of Proteasome Inhibitor

It is known that some cell extracts, such as rabbit reticulocyte or HeLa S-100 fraction, have 26S proteasome-dependent proteolytic activity [28,29]. Based on the presence of endogenous E1 and E2 ubiquitination and polyubiquitination in the wheat cell-free system, it is expected that the 26S proteasome activity will be very low (Fig. 2, 3 and 4). It was previously reported that the wheat germ extract had little 26S proteasome-dependent protein degradation activity [30]. Thus, we determined whether the wheat cell-free system contains active 26S proteasome. Using the crude recombinant proteins that formed polyubiquitin chains in this study, the polyubiquitination reaction was carried out in presence or absence of MG132, and accrual of the polyubiquitinated recombinant pro-

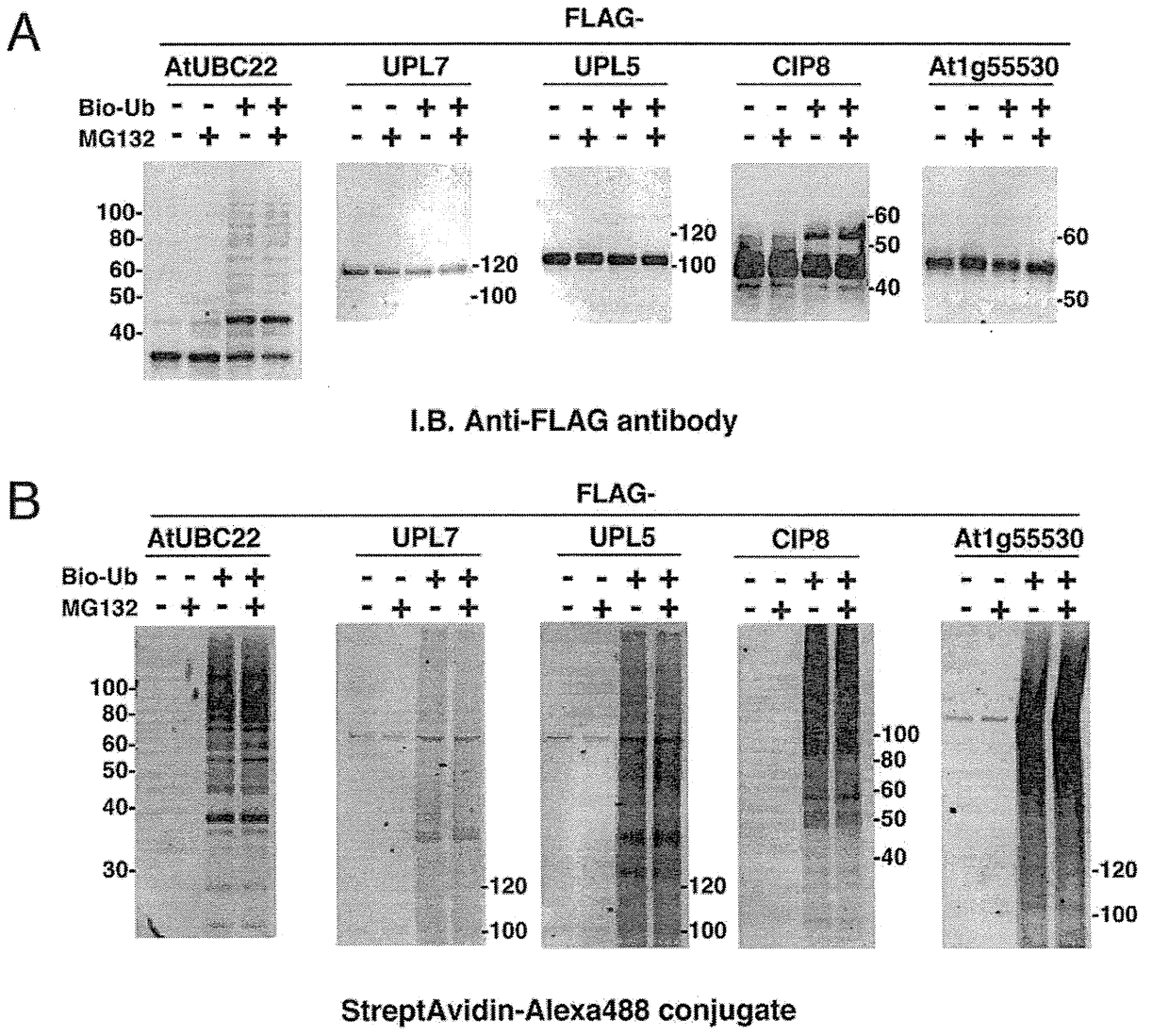

Figure 5
Effect of proteasome inhibitor on stability of polyubiquitinated proteins. Polyubiquitination assays of crude FLAG-tagged E2s and E3s were carried out in the presence or absence of biotinylated ubiquitin and 20 μM MG132. A, FLAG-tagged recombinant proteins were detected by immunoblot analysis using anti-FLAG antibody. B, Polyubiquitination chain formed by each recombinant protein was detected by Alexa488-conjugated streptavidin.

teins and its polyubiquitin chain was estimated. As shown in Fig 5, the amounts of UBC22, UPL5, UPL7 and At1g55530 (Fig. 5A) and of its polyubiquitin chains (Fig. 5B) were hardly altered by MG132 treatment. This result indicates that the proteolytic activity of the 26S proteasome in the wheat cell-free system was below the detection level. Thus, the wheat cell-free system could be suitable for ubiquitination analysis.

Discussion

The ubiquitin signal is an important protein modification in eukaryotes. Binding of a single ubiquitin to a target protein, mono-ubiquitination, is essential for membrane trafficking, protein functions and protein-protein interaction [7]. As for polyubiquitination, both Lys-48- and Lys-63-linked polyubiquitin chains have been well characterized in mammals and yeast. Lys-48 linked chains cause proteolysis of target proteins [6], and Lys-63 linked chains reg-

ulate signal transduction such as cellular localization of protein or protein-protein interactions [7]. In mammals, the multi-functional activities of NF-κB are regulated by the Lys-63 linked chain [31]. In plants, the function of the Lys-63 linked chain is still obscure. However, Arabidopsis E2 and its variants promote formation of the Lys-63 linked chain [32], suggesting that the Lys-63 linked chain in plant cells might also function similar to animal cells. Hence, comprehensive analysis of the ubiquitin-related plant proteins would open a door for elucidation of the plant ubiquitin pathway. In this study, we developed a simple and highly sensitive ubiquitination assay method by combination of the wheat cell-free protein synthesis system and luminescent detection. In general, *in vivo* protein production requires many time-consuming steps such as vector construction, cell culture and purification to obtain the recombinant protein. In contrast, this cell-free based luminescence method could analyze a large amount of ubiquitin reactions without these steps.

Using this method, we conveniently detected polyubiquitin chain formation of E2 and E3s by using two tagged ubiquitins (Fig. 1, 2, 3 and 4). The result of polyubiquitination analysis of the E2s obtained from luminescent-based detection method was verified by immunoblot analysis (Fig. 1). Our analysis also produced recombinant protein of HECT-type E3 ligases without truncation and detected their ubiquitin-conjugation and polyubiquitination activity by luminescent analysis (Fig. 2C and 2D). The ubiquitin-conjugation of UPL5 was not observed when a reductant was added to the reaction (data not shown), suggesting that UPL5 formed a thioester bond with ubiquitin. In addition, the model RING-type E3 CIP8 possessed high polyubiquitin formation activity without substrate, consistent with what was reported previously [26]. Crude recombinant CIP8 formed polyubiquitin chains in the absence of exogenous E1 and E2 (Fig. 3C and 3D), suggesting that the wheat cell-free system might include enough endogenous E1 and E2 activity. It was reported that wheat germ extracts have only a partial ubiquitin pathway [30]. Although the process to isolate wheat germ extract is different from the conventional methods [33], this report strongly supports the existence of endogenous ubiquitin pathway in our wheat cell-free system. Indeed, luminescent analysis using crude recombinant protein showed slight polyubiquitin chain formation even in absence of recombinant E3 (Fig. 2D, Fig. 3C and Fig. 4A, "E3-" lane), indicating that wheat cell-free system might include not only E1 and E2, but E3s or other factors that accelerates the polyubiquitin chain formation. Further, quantitative immunoblot analysis using anti-ubiquitin antibody showed that free ubiquitin was also present in wheat germ extract at a concentration of at least 10 nM (data not shown). This is similar to the ubiquitin concentration supplied in the *in vitro* assay. Although we developed a convenient screening method to detect E3 activity in this study, removal of the endogenous ubiquitin and ubiquitin related components such as E1, E2 and E3, would yield a more sensitive assay. However, wheat cell-free system does not have 26S proteasome proteolytic activity (Fig. 5), indicating that using crude recombinant protein is sufficient for *in vitro* ubiquitination assays.

By using this method, we found that a previously uncharacterized RING type E3, At1g55530, possessed high polyubiquitination activity without exogenous E1 and E2 proteins (Fig. 4). This result suggested that the method developed here is expected to find the activity of other unknown E3 ligases such as At1g55530. Despite having only 32% sequence similarity, the E3s CIP8 and At1g55530 showed similar biochemical functions. Polyubiquitin chains formed by CIP8 and At1g55530 elongated on themselves, while another report showed that polyubiquitin chains were formed on E2 before transferring them to substrates [34]. This reflects that the pattern of polyubiquitin chain formation differs between individual E3s and that the detailed mechanisms are still unknown. These studies suggest the importance of functional analysis using active recombinant proteins. Although we developed a simple screen using crude recombinant E3s in absence of exogenous E1 and E2 (Fig. 4), this method could not detect the activity of some E3 ligases that were unable to utilize endogenous ubiquitination components in wheat cell-free system. The polyubiquitination activity of At5g20910 recombinant protein, expressed in *E. coli* in the presence of AtUBC8 [25], was not active in our *in vitro* system (Fig. 4A), suggesting that in some cases exogenous E2 and/or other components are necessary additions. Such modifications to the ubiquitination assays detailed here would help elucidate the biochemical features of E3s (e.g., addition of recombinant E2s to reaction mixture could give us further information about the E2–E3 specificity, and of other E3 components would lead to the elucidation of structure of complex type E3 ligase such as SCF).

Conclusion

In this study, we found that the wheat cell-free system was an excellent expression system to produce recombinant protein efficiently and to carry out *in vitro* ubiquitination assays without the interference of proteolytic activity. Coupled with luminescent analysis, detection of these ubiquitin reactions in the crude translation reaction mixture was possible. Thus, this method should be helpful for solving the complicated ubiquitin pathway in plant.

Methods

Construction of DNA Templates for Transcription

We used RAFL as templates. DNA templates of E2s and E3s for transcription were constructed by "Split-Primer"

PCR as described previously [17]. Primers used in this study are summarized in Additional file 1. The first round of PCR was performed on each cDNA template using 10 nM of each of the following primers: a target protein specific primer (5'-CCACCCACCACCACCAatgnnnnnnnnn nnnnnnnn-3'; lowercase indicates the 5'-coding region of the target gene) and the AODA2306 primer. Then, a second round of PCR was carried out to construct the templates for protein synthesis using a portion (5 μl) of the first PCR mix, 100 nM SPu primer, 100 nM AODA2303 primer and 1 nM deSP6E02 primer. GST tags were used according to the methods we described previously [17]. The transcription templates of two HECT-type E3 ligases, UPL7 and UPL5, were generated as C-terminal FLAG-tagged proteins using the Gateway System® (Invitrogen, Carlsbad, CA, USA). Briefly, the ORF sequences of UPL7 and UPL5 were amplified by PCR with sense and antisense primers containing attB1 and FLAG-attB2 sequences, respectively. According to the manufacturer's instructions (Invitrogen), these DNA fragments were subcloned into pDONR221 vector by BP reaction and then inserted into the Gateway-based pEU vector (pEU-E01-GW) by LR reaction. Using these recombinant vectors as templates, PCR was carried out with 100 nM SPu primer and 100 nM AODA2303 primer and used as transcription templates.

Cell-free Protein Synthesis

In vitro transcription and cell-free protein synthesis were performed as described [18]. Transcript was made from each of the DNA templates mentioned above using the SP6 RNA polymerase. The synthetic mRNAs were then precipitated with ethanol and collected by centrifugation using a Hitachi R10H rotor. Each mRNA (usually 30–35 μg) was washed and transferred into a translation mixture. The translation reaction was performed in the bilayer mode [35] with slight modifications. The translation mixture that formed the bottom layer consisted of 60 A260 units of the wheat germ extract (CellFree Sciences, Yokohama, Japan) and 2 μg creatine kinase (Roche Diagnostics K. K., Tokyo, Japan) in 25 μl of SUB-AMIX® (CellFree Sciences). The SUB-AMIX® contained (final concentrations) 30 mM Hepes/KOH at pH 8.0, 1.2 mM ATP, 0.25 mM GTP, 16 mM creatine phosphate, 4 mM DTT, 0.4 mM spermidine, 0.3 mM each of the 20 amino acids, 2.7 mM magnesium acetate, and 100 mM potassium acetate. SUB-AMIX® (125 μl) was placed on the top of the translation mixture, forming the upper layer. After incubation at 16°C for 15 h, the synthesized proteins were confirmed by SDS-PAGE. For biotin labeling, 1 μl of crude biotin ligase (BirA) produced by the wheat cell-free expression system was added to the bottom layer, and 0.5 μM (final concentration) of D-biotin (Nacalai Tesque, Inc., Kyoto, Japan) was added to both upper and bottom layers, as described previously [22].

Purification of E2 and E3 Proteins

Purification of GST-tagged protein was carried out according to the procedure described previously [36] with slight modification. Crude GST-tagged recombinant protein (450 μl) produced by the cell-free reaction was precipitated with glutathione sepharose™ 4B (GE Healthcare, Buckinghamshire, UK). The recombinant proteins were eluted with PBS buffer containing 0.1 U of AcTEV protease (Invitrogen) in order to cleave the GST tag from the protein.

Detection of Polyubiquitination by the Luminescent Method

In vitro polyubiquitination assays were carried out in a total volume of 15 μl consisting of 20 mM Tris-HCl pH 7.5, 0.2 mM DTT, 5 mM $MgCl_2$, (10 μM zinc acetate in the assays for RING-type E3s only), 3 mM ATP, 1 mg/ml BSA, 25 nM biotinylated ubiquitin, 25 nM FLAG-tagged ubiquitin, 1 μl of recombinant E2 (purified or crude) and 1 μl of recombinant E3 (purified or crude) in the presence or absence of 0.05 μM rabbit E1 (Boston Biochem, Cambridge, MA, USA) at 30°C for 1 hr in a 384-well Optiplate (PerkinElmer, Boston, MA, USA). In accordance with the AlphaScreen IgG (ProteinA) detection kit (Perkin Elmer) instruction manual, 10 μl of detection mixture containing 20 mM Tris-HCl pH 7.5, 0.2 mM DTT, 5 mM $MgCl_2$, 5 μg/ml Anti-FLAG antibody (Sigma-Aldrich, St. Louis, MO, USA), 1 mg/ml BSA, 0.1 μl streptavidin-coated donor beads and 0.1 μl anti-IgG acceptor beads were added to each well of the 384 Optiplate followed by incubation at 23°C for 1 hr. Luminescence was analyzed by the AlphaScreen detection program.

Detection of Ubiquitinated E2 by Immunoblot Analysis

Crude biotinylated recombinant E2 proteins (40 μl) were used for the ubiquitin-conjugating assay in a total reaction volume of 50 μl containing 20 mM Tris-HCl pH 7.5, 0.2 mM DTT, 5 mM $MgCl_2$, 3 mM ATP and 4 μM FLAG-tagged ubiquitin (Sigma) for 3 hr at 30°C. The reaction products were purified by Streptavidin Magnesphere Paramagnetics particles (Promega, Madison, WI, USA). After washing the beads with PBS buffer, recombinant E2s were boiled in 15 μl of SDS sample buffer containing 50 mM Tris-HCl pH 6.8, 2% SDS, 10% glycerol and 0.2% bromophenol blue, and then separated from the magnet beads. The proteins were separated by SDS-PAGE and transferred to PVDF membrane (Millipore Bedford, MA, USA) according to standard procedures. The blots were detected by the ECL plus detection system (GE Healthcare) with anti-FLAG antibody (Sigma) according to the manufacturer's procedure.

Detection of Polyubiquitination by the Immunoblot Analysis

For polyubiquitination of HECT-type E3 ligases, crude FLAG-tagged UPL recombinant protein (20 μl) was ubiq-

uitinated in a total reaction volume of 50 μl consisting of 20 mM Tris-HCl pH 7.5, 0.2 mM DTT, 5 mM $MgCl_2$, 3 mM ATP, 4 μM biotinylated ubiquitin and 20 μl of crude recombinant AtUBC8 for 3 hr at 30°C. Then, recombinant UPL protein was gathered by anti-FLAG M2 agarose (Sigma). After washing the agarose with PBS buffer, the recombinant UPL protein was boiled in 15 μl of SDS sample buffer and then separated from beads by centrifugation. For polyubiquitination of RING-type E3 ligases, the assay was carried out in 10 μl of reaction mixture containing 20 mM Tris-HCl pH 7.5, 0.2 mM DTT, 5 mM $MgCl_2$, 10 μM zinc acetate, 3 mM ATP, 1 mg/ml BSA, 4 μM FLAG- or His-tagged ubiquitin, 1 μl of purified or crude recombinant E2 and 1 μl of purified or crude recombinant E3 at 30°C for 3 hr. Then, 5 μl of three-fold concentrated SDS sample buffer was added to the reaction mixture and boiled for 5 min. Proteins were separated by SDS-PAGE and transferred to Hybond-LFP PVDF membrane (GE Healthcare) according to standard procedures. Immunoblot analysis was carried out with anti-FLAG antibody (Sigma) or anti-His antibody (GE Healthcare) according to the procedure described above. When detecting biotinylated ubiquitin, blots were treated with 5 μg/ml Alexa488-conjugated streptavidin (Invitrogen) in PBS buffer. After washing with PBS containing 0.1% Tween-20, the blot was analyzed by a Typhoon Imager (GE Healthcare) using the 532 nm laser and 526 emission filters.

Polyubiquitination Assay with 26S Proteasome Inhibitor

Polyubiquitination reaction was carried out as same procedure described above except addition of MG132 (Calbiochem, San Diego, CA, USA) at a final concentration of 20 μM to reaction mixture. Then, the protein on blot was detected by immunoblot analysis with anti-FLAG antibody or Alexa488-conjugated streptavidin.

Authors' contributions

HT conceived the study and performed the experiments, and contributed to writing the manuscript. MS and KS provided RAFL cDNA clones. AN conceived the study. YE conceived the study and supervised the work. TS conceived and designed the study, supervised the work and contributed to writing the manuscript.

Additional material

Additional file 1

AGI code of Arabidopsis genes and primer sequences used in this study.

AGI code of Arabidopsis genes and primer sequences used in this study.
Click here for file
[http://www.biomedcentral.com/content/supplementary/1471-2229-9-39-S1.xls]

Acknowledgements

This work was partially supported by the Special Coordination Funds for Promoting Science and Technology by the Ministry of Education, Culture, Sports, Science and Technology, Japan (T. S. and Y. E.). We thank Michael Andy Goren for proofreading this manuscript.

References

1. Bai C, Sen P, Hofmann K, Ma L, Goebl M, Harper JW, Elledge SJ: **SKP1 Connects Cell Cycle Regulators to the Ubiquitin Proteolysis Machinery through a Novel Motif, the F-Box.** *Cell* 1996, **86(2)**:263-274.
2. Chen Z, Hagler J, Palombella VJ, Melandri F, Scherer D, Ballard D, Maniatis T: **Signal-induced site-specific phosphorylation targets IκBα to the ubiquitin-proteasome pathway.** *Genes Dev* 1995, **9(13)**:1586-1597.
3. Pickart CM: **Mechanisms underlying ubiquitination.** *Annu Rev Biochem* 2001, **70**:503-533.
4. Smalle J, Vierstra RD: **The ubiquitin 26S proteasome proteolytic pathway.** *Annu Rev Plant Biol* 2004, **55**:555-590.
5. Borden KL: **RING domains: master builders of molecular scaffolds?** *J Mol Biol* 2000, **295(5)**:1103-1112.
6. Glickman MH, Ciechanover A: **The ubiquitin-proteasome proteolytic pathway: destruction for the sake of construction.** *Physiol Rev* 2002, **82(2)**:373-428.
7. Schnell JD, Hicke L: **Non-traditional functions of ubiquitin and ubiquitin-binding proteins.** *J Biol Chem* 2003, **278(38)**:35857-35860.
8. Hofmann RM, Pickart CM: **Noncanonical MMS2-encoded ubiquitin-conjugating enzyme functions in assembly of novel polyubiquitin chains for DNA repair.** *Cell* 1999, **96(5)**:645-653.
9. Yin XJ, Volk S, Ljung K, Mehlmer N, Dolezal K, Ditengou F, Hanano S, Davis SJ, Schmelzer E, Sandberg G, Teige M, Palme K, Pickart C, Bachmair A: **Ubiquitin lysine 63 chain forming ligases regulate apical dominance in Arabidopsis.** *Plant Cell* 2007, **19(6)**:1898-1911.
10. Hicke L: **A new ticket for entry into budding vesicles – ubiquitin.** *Cell* 2001, **106(5)**:527-530.
11. Vierstra RD: **The ubiquitin/26S proteasome pathway, the complex last chapter in the life of many plant proteins.** *Trends Plant Sci* 2003, **8(3)**:135-142.
12. Nelson DC, Lasswell J, Rogg LE, Cohen MA, Bartel B: **FKF1, a Clock-Controlled Gene that Regulates the Transition to Flowering in Arabidopsis.** *Cell* 2000, **101(3)**:331-340.
13. Osterlund MT, Hardtke CS, Wei N, Deng XW: **Targeted destabilization of HY5 during light-regulated development of Arabidopsis.** *Nature* 2000, **405(6785)**:462-466.
14. Stone SL, Williams LA, Farmer LM, Vierstra RD, Callis J: **KEEP ON GOING, a RING E3 ligase essential for Arabidopsis growth and development, is involved in abscisic acid signaling.** *Plant Cell* 2006, **18(12)**:3415-3428.
15. Rosebrock TR, Zeng L, Brady JJ, Abramovitch RB, Xiao F, Martin GB: **A bacterial E3 ubiquitin ligase targets a host protein kinase to disrupt plant immunity.** *Nature* 2007, **448(7151)**:370-374.
16. Kraft E, Stone SL, Ma L, Su N, Gao Y, Lau OS, Deng XW, Callis J: **Genome analysis and functional characterization of the E2 and RING-type E3 ligase ubiquitination enzymes of Arabidopsis.** *Plant Physiol* 2005, **139(4)**:1597-1611.
17. Sawasaki T, Ogasawara T, Morishita R, Endo Y: **A cell-free protein synthesis system for high-throughput proteomics.** *Proc Natl Acad Sci USA* 2002, **99(23)**:14652-14657.
18. Sawasaki T, Gouda MD, Kawasaki T, Tsuboi T, Tozawa Y, Takai K, Endo Y: **The wheat germ cell-free expression system: methods for high-throughput materialization of genetic information.** *Methods Mol Biol* 2005, **310**:131-144.
19. Kobayashi T, Kodani Y, Nozawa A, Endo Y, Sawasaki T: **DNA-binding profiling of human hormone nuclear receptors via fluorescence correlation spectroscopy in a cell-free system.** *FEBS Lett* 2008, **582(18)**:2737-2744.
20. Seki M, Narusaka M, Kamiya A, Ishida J, Satou M, Sakurai T, Nakajima M, Enju A, Akiyama K, Oono Y, Muramatsu M, Hayashizaki Y, Kawai J, Carninci P, Itoh M, Ishii Y, Arakawa T, Shibata K, Shinagawa A, Shinozaki K: **Functional annotation of a full-length Arabidopsis cDNA collection.** *Science* 2002, **296(5565)**:141-145.
21. Kus B, Gajadhar A, Stanger K, Cho R, Sun W, Rouleau N, Lee T, Chan D, Wolting C, Edwards A, Bosse R, Rotin D: **A high throughput**

screen to identify substrates for the ubiquitin ligase Rsp5. *J Biol Chem* 2005, **280(33)**:29470-29478.
22. Sawasaki T, Kamura N, Matsunaga S, Saeki M, Tsuchimochi M, Morishita R, Endo Y: **Arabidopsis HY5 protein functions as a DNA-binding tag for purification and functional immobilization of proteins on agarose/DNA microplate.** *FEBS Lett* 2008, **582(2)**:221-228.
23. Bates PW, Vierstra RD: **UPL1 and 2, two 405 kDa ubiquitin-protein ligases from Arabidopsis thaliana related to the HECT-domain protein family.** *Plant J* 1999, **20(2)**:183-195.
24. Downes BP, Stupar RM, Gingerich DJ, Vierstra RD: **The HECT ubiquitin-protein ligase (UPL) family in Arabidopsis: UPL3 has a specific role in trichome development.** *Plant J* 2003, **35(6)**:729-742.
25. Stone SL, Hauksdóttir H, Troy A, Herschleb J, Kraft E, Callis J: **Functional analysis of the RING-type ubiquitin ligase family of Arabidopsis.** *Plant Physiol* 2005, **137(1)**:13-30.
26. Hardtke CS, Okamoto H, Deng XW: **Biochemical evidence for ubiquitin ligase activity of the Arabidopsis COP1 interacting protein 8 (CIP8).** *Plant J* 2002, **30(4)**:385-394.
27. Yamauchi K, Wada K, Tanji K, Tanaka M, Kamitani T: **Ubiquitination of E3 ubiquitin ligase TRIMa and its potential role.** *FEBS J* 2008, **275(7)**:1540-1555.
28. Waxman L, Fagan JM, Goldberg AL: **Demonstration of two distinct high molecular weight proteases in rabbit reticulocytes, one of which degrades ubiquitin conjugates.** *J Biol Chem* 1987, **262(6)**:2451-2457.
29. Chen ZJ, Parent L, Maniatis T: **Site-Specific Phosphorylation of IκBα by a Novel Ubiquitination-Dependent Protein Kinase Activity.** *Cell* 1996, **84(6)**:853-862.
30. Hatfield PM, Vierstra RD: **Ubiquitin-dependent proteolytic pathway in wheatgerm: Isolation of multiple forms of ubiquitin-activating enzyme, E1.** *Biochemistry* 1989, **28**:735-742.
31. Wu CJ, Conze DB, Li T, Srinivasula SM, Ashwell JD: **Sensing of Lys 63-linked polyubiquitination by NEMO is a key event in NF-κB activation.** *Nature Cell Biol* 2006, **8(4)**:398-406.
32. Yin XJ, Volk S, Ljung K, Mehlmer N, Dolezal K, Ditengou F, Hanano S, Davis SJ, Schmelzer E, Sandberg G, Teige M, Palme K, Pickart C, Bachmaira A: **Ubiquitin lysine 63 chain-forming ligases regulate apical dominance in Arabidopsis.** *Plant Cell* 2007, **19(6)**:1898-1911.
33. Madin K, Sawasaki T, Ogasawara T, Endo Y: **A highly efficient and robust cell-free protein synthesis system prepared from wheat embryos: Plants apparently contain a suicide system directed at ribosomes.** *Proc Natl Acad Sci USA* 2000, **97(2)**:559-564.
34. Li W, Tu D, Brunger AT, Ye Y: **A ubiquitin ligase transfers preformed polyubiquitin chains from a conjugating enzyme to a substrate.** *Nature* 2007, **446(7133)**:333-337.
35. Sawasaki T, Hasegawa Y, Tsuchimochi M, Kamura N, Ogasawara T, Kuroita T, Endo Y: **A bilayer cell-free protein synthesis system for high-throughput screening of gene products.** *FEBS Lett* 2002, **514(1)**:102-105.
36. Masaoka T, Nishi M, Ryo A, Endo Y, Sawasaki T: **The wheat germ cell-free based screening of protein substrates of calcium/calmodulin-dependent protein kinase II delta.** *FEBS Lett* 2008, **582(13)**:1795-1801.

FEBS Letters 583 (2009) 1243–1250

journal homepage: www.FEBSLetters.org

Requirement for microtubule integrity in the SOCS1-mediated intracellular dynamics of HIV-1 Gag

Mayuko Nishi [a,b], Akihide Ryo [a,b,*], Naomi Tsurutani [c], Kenji Ohba [a], Tatsuya Sawasaki [d], Ryo Morishita [d], Kilian Perrem [e], Ichiro Aoki [b], Yuko Morikawa [c], Naoki Yamamoto [a,*]

[a] AIDS Research Center, National Institute of Infectious Diseases, 1-23-1 Toyama, Shinjuku-ku, Tokyo, Japan 162-8640, Japan
[b] Department of Pathology, Yokohama City University School of Medicine, 3-9 Fuku-ura, Kanazawa-ku, Yokohama 236-0004, Japan
[c] Kitasato Institute for Life Sciences, Kitasato University, Shirokane 5-9-1, Minato-ku, Tokyo 108-8641, Japan
[d] Cell Free Science and Research Center, Ehime University, Ehime 790-8577, Japan
[e] CSIRO, P.O. Box 225, Dickson ACT 2602, Australia

ARTICLE INFO

Article history:
Received 8 December 2008
Revised 16 March 2009
Accepted 18 March 2009
Available online 25 March 2009

Edited by Kaspar Locher

Keywords:
HIV
Host factor
Suppressor of cytokine signaling 1
Microtubule
Ubiquitin
Trafficking

ABSTRACT

Suppressor of cytokine signaling 1 (SOCS1) is a recently identified host factor that positively regulates the intracellular trafficking and stability of HIV-1 Gag. We here examine the molecular mechanism by which SOCS1 regulates intercellular Gag trafficking and virus particle production. We find that SOCS1 colocalizes with Gag along the microtubule network and promotes microtubule stability. SOCS1 also increases the amount of Gag associated with microtubules. Both nocodazole treatment and the expression of the microtubule-destabilizing protein, stathmin, inhibit the enhancement of HIV-1 particle production by SOCS1. SOCS1 facilitates Gag ubiquitination and the co-expression of a dominant-negative ubiquitin significantly inhibits the association of Gag with microtubules. We thus propose that the microtubule network plays a role in SOCS1-mediated HIV-1 Gag transport and virus particle formation.

Structured summary:
MINT-7014185: *Gag* (uniprotkb:P05888) and *SOCS1* (uniprotkb:O15524) *colocalize* (MI:0403) by *cosedimentation* (MI:0027)
MINT-7014239: *Cullin 2* (uniprotkb:Q13617) *physically interacts* (MI:0218) with *RelA* (uniprotkb:Q04206), *RBX1* (uniprotkb:P62877), *SOCS1* (uniprotkb:O15524), *elongin B* (uniprotkb:Q15369) and *elongin C* (uniprotkb:Q15370) by *pull-down* (MI:0096)
MINT-7014046: *gag* (uniprotkb:P05888), *SOCS1* (uniprotkb:O15524) and *tubulin alpha* (uniprotkb:Q13748) *colocalize* (MI:0403) by *fluorescence microscopy* (MI:0416)
MINT-7014269: *tubulin alpha* (uniprotkb:Q13748) *physically interacts* (MI:0218) with *Gag* (uniprotkb:P05888) by *anti tag coimmunoprecipitation* (MI:0007)
MINT-7014036: *tubulin alpha* (uniprotkb:Q13748) and *SOCS1* (uniprotkb:O15524) *colocalize* (MI:0403) by *fluorescence microscopy* (MI:0416)
MINT-7014201: *Cullin 2* (uniprotkb:Q13617) *physically interacts* (MI:0218) with *RBX1* (uniprotkb:P62877), *SOCS1* (uniprotkb:O15524), *elongin B* (uniprotkb:Q15369) and *elongin C* (uniprotkb:Q15370) by *pull-down* (MI:0096)
MINT-7014257: *Gag* (uniprotkb:P05888) *physically interacts* (MI:0218) with *Ubiquitin* (uniprotkb:P62988) by *anti tag coimmunoprecipitation* (MI:0007)
MINT-7014221: *Cullin 2* (uniprotkb:Q13617) *physically interacts* (MI:0218) with *Gag* (uniprotkb:P05888), *elongin C* (uniprotkb:Q15370), *elongin B* (uniprotkb:Q15369), *SOCS1* (uniprotkb:O15524) and *RBX1* (uniprotkb:P62877) by *pull-down* (MI:0096)

1. Introduction

The human immunodeficiency virus 1 (HIV-1) employs multistep and multi-factorial processes for producing progeny viruses during infection [1,2]. Virus must utilize the intrinsic transport machinery of the infected host cells to enable the active transport

Abbreviations: HIV, human immunodeficiency virus; SOCS1, Suppressor of cytokine signaling 1; KIR, kinase inhibitory region; MTOC, microtubule organizing center; Ub, ubiquitin; VLP, virus-like particle

* Corresponding authors. Address: AIDS Research Center, National Institute of Infectious Diseases, 4-7-1 Gakuen, Musashimurayama, Tokyo 208-0011, Japan (A. Ryo). Fax: +81 42 563 6291.
E-mail addresses: aryo@nih.go.jp (A. Ryo), nyama@nih.go.jp (N. Yamamoto).

0014-5793/$36.00 © 2009 Federation of European Biochemical Societies. Published by Elsevier B.V. All rights reserved.
doi:10.1016/j.febslet.2009.03.041

of viral proteins [3,4]. Several recent studies have identified cellular factors that modulate HIV-1 Gag trafficking and localization. These include AP-3δ, POSH, HP68, GGA and Trim22 [5–9]. Moreover, phosphatidylinositol-(4,5)-bisphosphate (PIP2) has been shown to control the targeting of Gag to the plasma membrane [10]. These findings point to a critical role of host cell factors in Gag assembly and release, but the precise molecular functions of these factors and the specific timing of their roles in this process remain largely unknown.

We recently reported that the suppressor of cytokine signaling 1 (SOCS1) is an inducible host factor during HIV-1 infection and plays an important role in the intracellular trafficking of Gag to the plasma membrane, resulting in the efficient production of HIV-1 particles [11]. Moreover, we have further shown that the function of SOCS1 in Gag trafficking and HIV-1 particle production is not principally due to the suppression of interferon/cytokine signaling, but is mediated via its interaction with the HIV-1 Gag polyprotein [11]. Importantly, the targeted depletion of SOCS1 results in the mistargeting and degradation of Gag in lysosomes, leading to a significant decrease in virus particle production [11].

In our current study, we have utilized SOCS1 as a molecular tool to further reveal the molecular mechanisms underlying the intracellular transport of HIV-1 Gag during viral infection. We reveal from our findings that SOCS1 regulates the Gag trafficking process via the microtubule-dependent cellular machinery. Furthermore, we find that Gag is also regulated by a ubiquitin signaling pathway which is accompanied by Gag ubiquitination. These findings shed new light on the mechanisms involved in the intracellular transport of HIV-1 Gag and provide important clues for the design of future novel therapeutic interventions against AIDS and related disorders.

2. Materials and methods

2.1. Antibodies

Antibodies (Abs) and fluorescent reagents were obtained from the following sources: rabbit polyclonal anti-myc (A-14) and rabbit polyclonal anti-SOCS1 (H-93) Abs (Santa Cruz Biotechnology); rabbit polyclonal anti-SOCS1 (Zymed Laboratories); mouse monoclonal anti-FLAG (M2), anti-α-tubulin, anti-acetylated-α-tubulin and anti-γ-tubulin Abs (Sigma, St. Louis, MO); rabbit polyclonal anti-stathmin antibody (Calbiochem); mouse monoclonal anti-myc antibody (9B11, Cell Signaling Technology); mouse monoclonal anti-cytokeratin 7, cytokeratin 18, vimentin and HIV-p24 Ab (Dako Cytomation). Immunoblotting, immunoprecipitation and immunofluorescent analyses were performed as described previously [11].

2.2. Plasmids and sequences

Expression constructs for SOCS1 have been described previously [12]. HIV-1 Gag constructs have also been described previously [13]. Stathmin cDNA was amplified by RT-PCR from a human kidney cDNA library using the primers 5′-AGCAAG CTTGCCACCATGGCTTCTTCTGATATCCAGG-3′ and 5′-GACGGATCC GTCAGCTTCAGTCTCGTCAG-3′ and then subcloned into the pcDNA3.1 vector. pcDNA3.1-myc-ubiquitin and its mutants were generated by PCR as described previously [14]. The siRNA sequences were as follows: SOCS1-siRNA, GGCCAGAACCTT CCTCCTCTT; control-siRNA, TCGTATGTTGTGTGGAATT. All expression constructs were validated by sequencing.

2.3. Microtubule-associated protein spin-down assays

Microtubule-associated proteins were collected using a microtubule-associated protein spin-down assay kit (Cytoskeleton, BK029) according to the manufacturer's instructions. Briefly, 293T cells were lysed in 0.5 ml of PEM buffer (80 mM PIPES, pH 6.9, 0.3% Triton X-100, 1 mM EGTA, 1 mM GTP, GTP, 1 mM $MgCl_2$) supplemented with 1 mM phenylmethylsulfonyl fluoride, 5 μg/ml leupeptin, 2 μg/ml aprotinin, 1 mM sodium orthovanadate, and 5 mM NaF. Cell lysates were incubated with taxol-stabilized microtubules, followed by ultracentrifuge at 100000×*g* for 40 min at 25 ℃.

2.4. Cell culture

The 293T, COS-1, COS-7, HeLa and HOS cell lines and mouse embryonic fibroblasts (MEFs) were cultured in DMEM supplemented with 10% FBS. SOCS1−/− MEF cells were cultured as described previously [12].

2.5. In vitro interaction analysis

The in vitro interaction between HIV-1 Gag and the SOCS1-E3 complex was analyzed as follows: ^{14}C-labeled recombinant proteins (SOCS1, elongin B/C, Rbx1, biotin labeled cullin 2, and HIV-1 Gag) were synthesized in a wheat germ cell-free system as described previously [15]. The synthesized proteins were subsequently incubated in 120 μl of reaction buffer (50 mM Tris–HCl, pH 7.6, 50 mM $MgCl_2$, 500 mM CH_3COOK, 0.1 mM DTT and 1 mg/ml BSA) and streptavidin magnetic beads (Promega, Madison, WI) at 23 °C for 1 h. The precipitated proteins were then washed three times with reaction buffer and subjected to autoradiography.

3. Results

3.1. SOCS1 aligns with microtubule forming fibrous structures

SOCS1 has been shown previously to localize at both the perinuclear region and the microtubule organizing center (MTOC) [16]. This finding indicated the possible involvement of the microtubule network in the regulation of Gag by SOCS1. We thus addressed whether the Gag transport system is in fact mediated by microtubule integrity and if SOCS1 enhances this process. Immunofluorescent analysis with α-tubulin antibodies revealed that endogenous SOCS1 forms punctate structures that align with the microtubule network (Fig. 1A). Importantly, these signals were completely abolished when the cells were stained with anti-SOCS1 antibodies that had been pre-absorbed with recombinant SOCS1 protein, confirming the specificity of this antibody (Fig. 1B). Parallel experiments revealed that SOCS1 does not colocalize with other cytoskeletal components such as actin or intermediate filaments (Fig. 1C).

3.2. SOCS1 promotes microtubule stability

Given our finding that SOCS1 can tightly associate with microtubules, we next addressed whether SOCS1 affects microtubule stability. Stabilized microtubules are frequently enriched in tubulin that has undergone post-translational modifications such as acetylation [17]. We found that the high expression of SOCS1 results in higher amounts of acetylated microtubules in three different cell lines when compared with control cells (Fig. 2A) and that this trend is dose-dependent in COS-7 cells (Fig. 2B). On the other hand, SOCS1−/− mouse embryonic fibroblasts (MEFs) exhibited lower levels of acetylated α-tubulin compared with wild-type MEFs (Fig. 2C). These results indicate that SOCS1 does indeed contribute to the stabilization of microtubules.

Mammalian cells usually possess a population of microtubules that are resistant to the depolymerization effects of microtubule disorganizing reagents. We thus addressed whether SOCS1 impacts

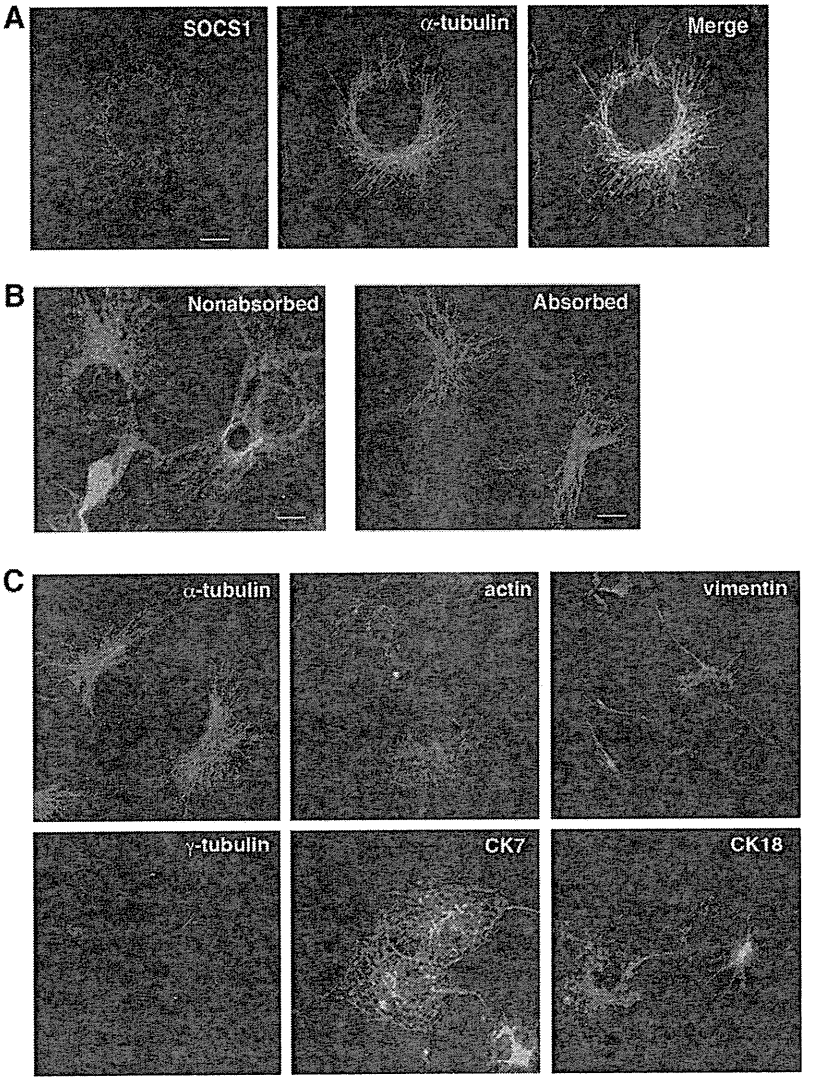

Fig. 1. SOCS1 colocalizes with microtubule forming fibrous structures. (A) COS-1 cells were fixed with 3% formaldehyde followed by 100% cold methanol, and then co-immunostained with polyclonal antibodies targeting SOCS1 (red) and monoclonal antibodies targeting α-tubulin (green). Cells were then analyzed by confocal microscopy. Scale bar, 10 μm. (B) COS-1 cells were immunostained with anti-α-tubulin monoclonal antibodies together with anti-SOCS1 polyclonal antibodies that had either been non-absorbed or pre-absorbed with GST-SOCS1 proteins. This was followed by confocal microscopy. Scale bar, 10 μm. (C) COS-1 cells were fixed with 3% formaldehyde followed by 100% cold methanol, then co-immunostained with polyclonal antibodies targeting SOCS1 (red) and monoclonal antibodies targeting various cytoskeletal components (green). Cells were then analyzed by confocal microscopy.

upon this property in this subpopulation of microtubules in COS-7 cells. The cells were transfected with either SOCS1 or control vector and then treated with 1 μM colchicine for 12 h to fully depolymerize the microtubules. Immunostaining with antibodies against acetylated α-tubulin showed that the SOCS1 expressing cells contained more polymerized microtubules compared with the control cells (Fig. 2D). These results indicate that SOCS1 might contribute to the microtubule stability required for Gag trafficking via this network.

3.3. SOCS1 enhances the association of HIV-1 Gag with microtubules

We next investigated the sub-cellular localization of HIV-1 Gag with SOCS1 and microtubules. COS-1 cells were transfected with Gag-GFP and after 24 h were fixed with 3% formaldehyde, followed by 100% cold methanol. The cells were then immunostained with anti-SOCS1 and anti-α-tubulin antibodies. Consistent with our earlier results, confocal microscopic analysis revealed that SOCS1 can form dotted filamentous structures in the cytoplasm along the microtubules, and that HIV-1 Gag colocalizes with these SOCS1 puncta (Fig. 3A).

To next determine whether cellular SOCS1 and Gag can together mechanically bind microtubules, and thus whether SOCS1 expression has any impact upon the interaction between Gag and microtubules, we performed microtubule pull-down analysis. 293T cells were transfected with either Gag-FLAG, myc-SOCS1, or a combination of these two plasmids, and the lysates from these transfected cells were subsequently incubated with taxol-stabilized microtubules and centrifuged to pellet the microtubule-associated proteins. The pellet fractions were then subjected to immunoblotting using either anti-myc or anti-FLAG antibodies. SOCS1 was found to be co-sedimented with microtubules irrespective of whether Gag had been co-transfected (Fig. 3B). The quantities of microtubule-bound Gag in the pellet fraction, however, were significantly increased when SOCS1 was co-transfected (Fig. 3B). These results together indicate that SOCS1 is itself a microtubule binding protein that may also mediate the interaction between HIV-1 Gag and microtubules.

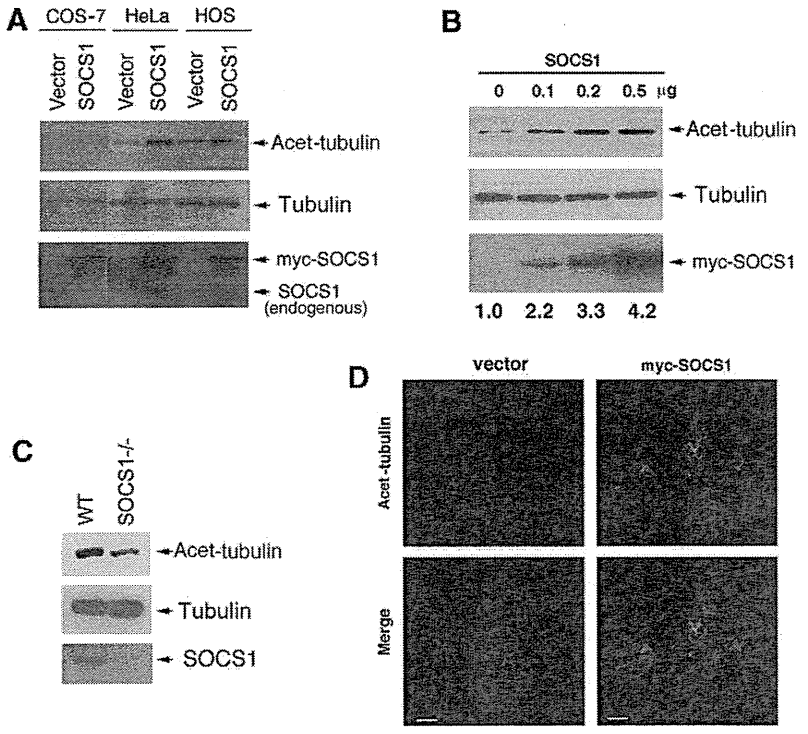

Fig. 2. SOCS1 enhances microtubule stability. (A) COS-7, HeLa or HOS cells were transfected with either empty vector or myc-SOCS1 for 48 h. Cell lysates were then subjected to immunoblotting analysis with antibodies against α-tubulin, acetylated α-tubulin or SOCS1. (B) COS-7 cells were transfected with various amounts of myc-SOCS1 as in (A). Cell lysates were then subjected to immunoblotting analysis with anti-α-tubulin, anti-acetylated-α-tubulin or anti-myc antibodies. Numerical values below the blots indicate acetylated α-tubulin signal intensities normalized by the unmodified α-tubulin intensity derived by densitometry. (C) Exponentially growing wild-type MEFs or SOCS1−/− MEFs were lysed and the cell lysates were immunoblotted with antibodies against α-tubulin, acetylated α -tubulin or SOCS1. (D) COS-7 cells were co-transfected with empty vector or myc-SOCS1, and then treated with colchicine (1 μM) for 12 h to depolymerize the microtubules. Cells were then fixed and immunostained with both anti-acetylated-α-tubulin (green) or anti-myc (red) antibodies and then stained with 4′,6-diamino-2-phenylindole (DAPI, blue), followed by confocal microscopy. Scale bar, 10 μm.

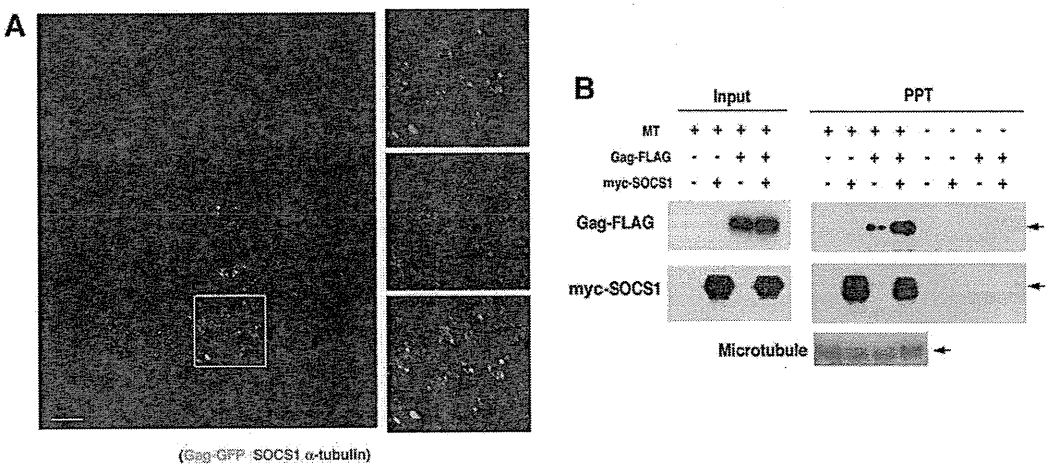

Fig. 3. SOCS1 enhances HIV-1 Gag associated with microtubules. (A) COS-1 cells transiently transfected with HIV-1 Gag-GFP were co-immunostained with antibodies targeting endogenous SOCS1 (red) and microtubules (α-tubulin, blue). The inset indicates the area shown at higher magnification in the right hand panels which reveal the colocalization of Gag-GFP with SOCS1 along the microtubules. Scale bar, 10 μm. (B) Cosedimentation of SOCS1 and HIV-1 Gag with polymerized microtubules. 293T cells were transfected with the indicated plasmids for 36 h. Cell lysates were then incubated with taxol-stabilized microtubules or control buffer and separated into precipitate (PPT) and supernatant fractions. Precipitate fractions were subjected to immunoblotting analysis with anti-myc or anti-FLAG antibodies.

3.4. Microtubule integrity is required for SOCS1 to function in HIV-1 particle formation

Our results shown above indicated that SOCS1 mediates the association of HIV-1 Gag with the microtubule networks. We next examined therefore whether SOCS1-mediated Gag trafficking, and the resultant HIV-1 particle production, are dependent upon an intact microtubule network. 293T cells were transfected with the HIV-1 molecular clone pNL4-3 and co-transfected with either empty vector alone or myc-SOCS1. After 24 h, the cells were washed with PBS and then cultured in the presence or absence of nocodazole for a further 6 h. Subsequent measurement of the p24 antigen levels in the cell supernatant by ELISA revealed nocodazole treatment significantly inhibited the enhancement of HIV-1 particle production in SOCS1-transfected cells more dramatically than in vector control transfected cells, and that this was

dose-dependent (Fig. 4A). Consistent with these results also, SOCS1 localization was observed to be significantly altered by nocodazole treatment, i.e. from a dotted filamentous structure along the microtubules to diffuse and larger aggregations in the cytoplasm (Fig. 4B). The use of trypan blue dye exclusion confirmed that cell viability was not affected by the nocodazole treatment (Fig. 4C).

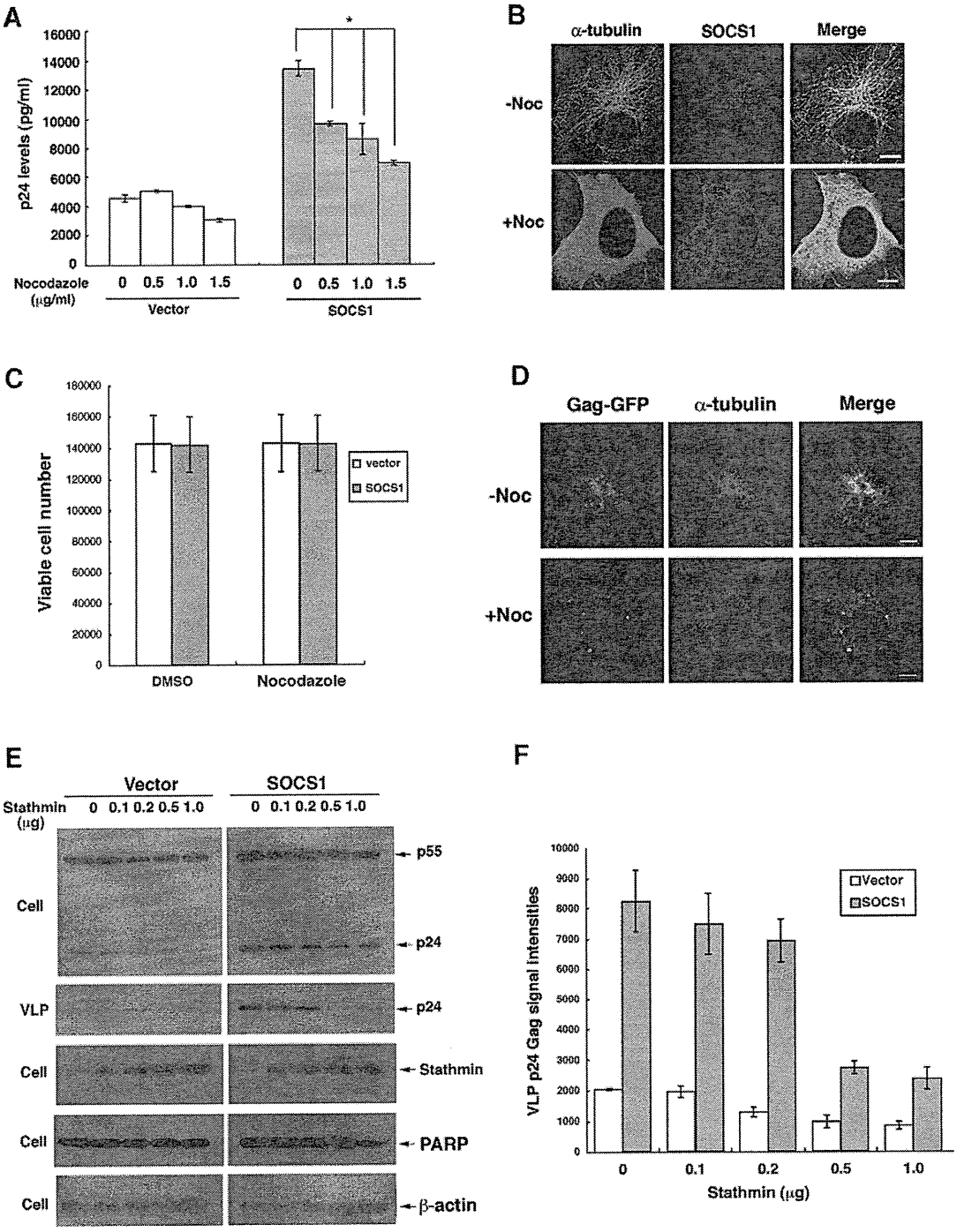

Fig. 4. Microtubule integrity is required for SOCS1 to function in HIV-1 particle formation. (A) 293T cells were transfected with pNL4-3, and co-transfected with either empty vector alone (Vector) or myc-SOCS1. After 24 h, cells were washed with PBS and then cultured with fresh media including the indicated concentrations of nocodazole for 6 h. Supernatant p24 antigen levels were measured by p24 ELISA . The data shown are the average ± S.D. of three independent experiments. $^{*}P \leqslant 0.05$, by the Student's *t*-test. (B and C) Mislocalization of SOCS1 in cells treated with nocodazole. COS-1 cells were treated with vehicle only or with nocodazole (2 μg/ml) for 6 h. Cells were then fixed and immunostained with both anti-SOCS1 (red) and anti-α-tubulin (green) antibodies, followed by confocal microscopy (B). Scale bar, 10 μm. The numbers of viable cells were calculated by trypan blue dye exclusion (C). (D) COS-1 cells transfected with Gag-GFP were treated with vehicle only or with nocodazole (2 μg/ml) for 6 h followed by immunostaining with anti-α-tubulin (red) antibody. Scale bar, 10 μm. (E and F) 293T cells were transfected with pNL4-3 and either vector or SOCS1, and co-transfected with various amounts of stathmin. At 36 h after transfection, cell lysate and supernatant virus-like particle (VLP) were processed for immunoblotting analysis with anti-p24, anti-PARP, anti-β-actin or anti-stathmin antibodies (E). VLP p24 Gag signal intensities, derived by densitometry, are shown in (F).

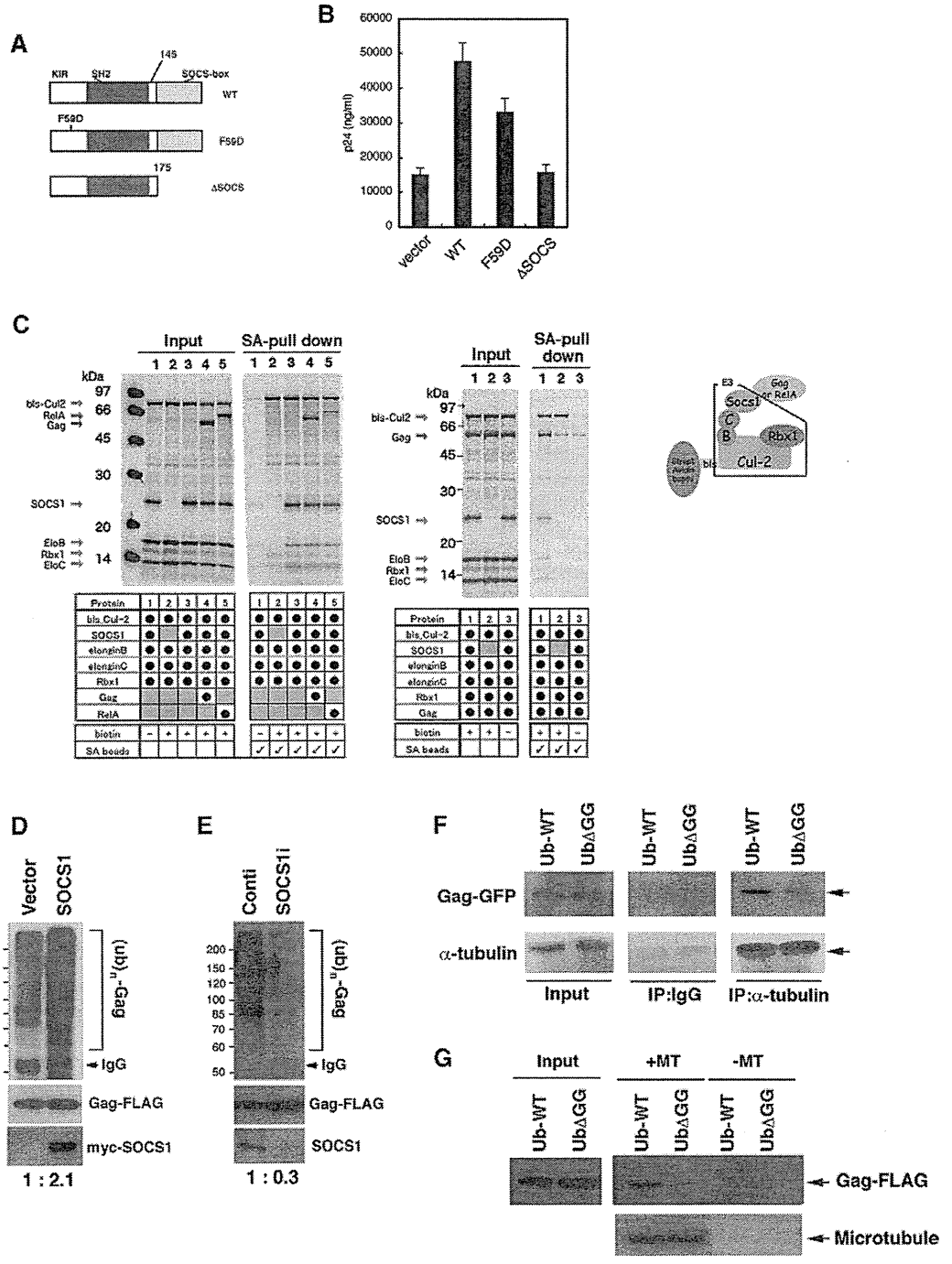

Fig. 5. SOCS1 enhances the ubiquitination of HIV-1 Gag and this affects the association of Gag with the microtubules. (A) Schematic represenation of SOCS1 mutants. (B) 293T cells were transfected with pNL4-3 and co-transfected with control vector, wild-type SOCS1 (WT), SOCS1-F59D mutant or ΔSOCS-box mutant. After 48 h, the p24 levels in the cell supernatants were measured by ELISA. (C) HIV-1 Gag associates with the ubiquitin ligase complex of SOCS1 in vitro. ^{14}C-labeled proteins (SOCS1, biotin labeled Cullin2, elongin B/C, Rbx1, HIV-1 Gag and RelA) were synthesized using a wheat germ cell-free system. Purified proteins were incubated in the indicated combinations for 1 h and subjected to co-purification with streptavidin magnetic beads. Captured proteins were then separated by SDS–PAGE followed by autoradiography. (D) 293T cells were co-transfected with Gag-FLAG, myc-tagged ubiquitin, and either empty vector (Vector) or SOCS1 expression construct. After 48 h, cells were lysed and denatured by boiling them in 1% SDS lysis buffer and diluted to RIPA buffer conditions, and Gag-FLAG proteins were immunoprecipitated (IP) with anti-FLAG antibody and processed for anti-myc immunoblotting to detect ubiquitinated Gag. Ubn, polyubiquitinated. Numerical values below blot indicates the relative levels of ubiquitinated Gag normalized by the amount of total Gag. (E) 293T cells were co-transfected with Gag-FLAG, myc-tagged ubiquitin, and either control-siRNA or SOCS1-siRNA. After 48 h, cell lysates were immunoprecipitated with anti-FLAG antibody and processed for anti-myc immunoblotting to detect ubiquitinated Gag. Ubn, polyubiquitinated. Numerical values below blot indicates the relative levels of ubiquitinated Gag normalized by the amount of total Gag. (F) 293T cells were transfected with Gag-GFP and SOCS1, and co-transfected with either myc-Ub-WT or myc-UbΔGG. After 24 h, cell lysates were harvested and subjected to immunoprecipitation analysis with anti-α-tubulin antibody or non-immunized mouse IgG (IgG) followed by immunoblotting analysis with the indicated antibodies. (G) 293T cells were transfected with Gag-FLAG and SOCS1, and co-transfected with either myc-Ub-WT or myc-UbΔGG. After 24 h, cell lysates were harvested and then incubated with taxol-stabilized microtubules (+MT) or control buffer (−MT), and separated into precipitate and supernatant fractions. Precipitate fractions were collected and then subjected to immunoblotting analysis with either anti-FLAG or anti-α-tubulin (microtubule) antibodies.

Furthermore, a parallel experiment revealed that the Gag-GFP puncta formed larger aggregations in the cytoplasm upon nocodazole treatment (Fig. 4D).

To further delineate the role of microtubule integrity in HIV-1 particle formation, we next performed experiments in which we co-transfected SOCS1 and pNL4-3 with or without the microtubule-destabilizing protein stathmin. Stathmin expression efficiently blocked the effects of SOCS1 upon HIV-1 particle formation in a dose-dependent manner (Fig. 4E and F). Cell viability was not strongly affected as revealed by immunoblotting analysis of either poly (ADP-ribose) polymerase (PARP) or β-actin (Fig. 4E). Our findings together indicate therefore that microtubule integrity may be required for SOCS1 to function in Gag assembly and release.

3.5. SOCS1 facilitates the ubiquitination of HIV-1 Gag

Our previous study has revealed that the SOCS-box of SOCS1 is required for both HIV-1 particle production and the enhancement of Gag association with microtubules [11]. The mechanism by which SOCS1 inhibits cytokine signaling is mediated by the inhibition of kinase activity through its N-terminal kinase inhibitory region (KIR) [18]. We next examined whether SOCS1 mutants lacking the function of either KIR (SOCS1-F59D) or SOCS-box (ΔSOCS) affected virus particle production. Our ELISA results indicate that the SOCS-box deletion mutant (ΔSOCS) of SOCS1 fails to promote virus production, whereas the KIR mutant, F59D, of SOCS1 partially enhances HIV-1 particle production when co-transfected with pNL4-3 in 293T cells (Fig. 5A and B). These data again suggest that the function of SOCS1 in HIV-1 particle production is not principally due to the suppression of interferon/cytokine signaling, but is mediated by its direct interaction with the HIV-1 Gag via the function of the SOCS-box.

The SOCS-box-mediated function of SOCS1 is chiefly exerted via its ubiquitin ligase activity [19]. Indeed, several reports have demonstrated that Gag ubiquitination is related to its membrane association and particle release, although the function of HIV-1 Gag ubiquitination remains unclear [20,21]. We thus explored the possibility that SOCS1 modulates the ubiquitination of HIV-1 Gag, leading to enhanced virus particle formation. We initially examined the specific interaction of HIV-1 Gag with the SOCS1-E3 ligase complex. Purified SOCS1 and its E3 component proteins (biotinylated-Cullin 2, elongin B/C and Rbx1) in addition to HIV-1 Gag were synthesized in a wheat germ cell-free system and then subjected to pull-down assays using streptavidin coated magnetic beads. We found that Gag was co-purified with a SOCS1-E3 complex comprising SOCS1-elongin B/C-Rbx1-Cullin2 in a similar manner to RelA, a previously reported SOCS1 binding protein (Fig. 5C, left). Significantly, in the absence of SOCS1, both elongin B and C were not co-purified with Cullin 2 probably due to the unsteady condition of the E3 complex without SOCS1, and the amount of bound Gag was also reduced (Fig. 5C, right).These result indicate that the SOCS1-E3 complex associates with HIV-1 Gag and may promote its ubiquitination.

We next addressed whether SOCS1 affects the ubiquitination of HIV-1 Gag. Immunoprecipitation analysis with cells co-transfected with Gag-FLAG and myc-tagged ubiquitin, with or without SOCS1 co-transfection, revealed that SOCS1 overexpression significantly enhances the ubiquitination of the Gag protein (Fig. 5D). In contrast, the targeted depletion of SOCS1 by siRNA significantly reduced the amount of ubiquitinated Gag (Fig. 5E). These results indicate that SOCS1 could indeed be a potent ubiquitin ligase for HIV-1 Gag.

To clarify the biological significance of Gag ubiquitination via SOCS1, we performed an experiment using a dominant-negative ubiquitin construct lacking two C-terminal glycines (residues 75–76). This mutant ubiquitin (UbΔGG) cannot become conjugated to target substrates, but can bind noncovalently to ubiquitin interacting domains [14]. By immunoprecipitation analysis we revealed that the levels of HIV-1 Gag associated with microtubules were significantly reduced in cells expressing UbΔGG, as compared with those expressing wild-type ubiquitin (Ub-WT) (Fig. 5F). This trend was further revealed by a microtubule sedimentation experiment showing that the expression of UbΔGG reduced the amount of Gag associated with microtubules when compared with the expression of Ub-WT (Fig. 5G). These results together indicate a link between ubiquitin signaling and the microtubule-mediated Gag dynamics involved with HIV-1 particle formation.

4. Discussion

In our current study, we report that microtubule integrity is required for SOCS1 to facilitate Gag trafficking and virus particle production. We demonstrate from our experiments that (1) SOCS1 colocalizes with HIV-1 Gag along microtubules; (2) both SOCS1 and HIV-1 Gag are co-purified with microtubules and SOCS1 can augment the association of Gag with microtubules; (3) an intact microtubule network is required for the function of SOCS1 during Gag trafficking; (4) SOCS1 facilitates Gag ubiquitination; and (5) Gag association with the microtubules is significantly reduced when a dominant-negative Ub mutant is overexpressed. These results together indicate that SOCS1 can regulate the trafficking and stability of HIV-1 Gag via the microtubule-related cellular machinery, which may be in turn enhanced by Gag ubiquitination.

SOCS1 was identified initially as a negative regulator of signaling downstream of cytokines [22–24] and has been shown to localize at both the perinuclear region and the microtubule organizing center (MTOC) in cells [16]. We show from our current data that SOCS1 also forms dotted filamentous structures in the cytoplasm emanating from the perinuclear region, including the MTOC, to the cell periphery. A recent report has also indicated that Gag colocalizes at the MTOC with HIV-1 RNA and is subsequently transported to the cell periphery [25]. These observations together indicate that SOCS1 might facilitate the trafficking of HIV-1 Gag from the MTOC toward the plasma membrane by utilizing the intrinsic transport machinery of infected host cells.

The plus-end directed transport system along the microtubules could provide a means for the targeting of virus capsid proteins to the site of virus assembly and budding in the vicinity of the plasma membrane [26]. This ante-grade transport system is utilized by several viruses, such as herpes simplex virus type 1 (HSV-1), vaccinia virus and African swine fever virus (ASFV) [26–29]. Significantly, we have demonstrated in our present study that HIV-1 can utilize the microtubule-dependent transport mechanism, which may in turn be enhanced by SOCS1. Consistent with this notion, Leblanc et al. have demonstrated previously using a monoclonal antibody raised against unprocessed Gag that intracellular Gag puncta can travel along microtubules [30]. Our current microtubule pull-down analyses also clearly indicate that SOCS1 associates with Gag on microtubules and can enhance this interaction. This in turn might accelerate the intracellular trafficking of Gag to the plasma membrane along these structures, although the topological details are still unknown. Consistent with this observation, a plus-end microtubule motor KIF4 has been shown previously to associate with HIV-1 Gag and to enhance Gag trafficking [31,32]. These results further demonstrate the relevance of microtubule network in the trafficking of the HIV-1 Gag.

The involvement of the microtubule cytoskeleton in Gag assembly and HIV-1 particle egress is somewhat controversial [3,26,33,34]. However, several reports have presented convincing data to indicate the importance of this network in HIV-1 assembly

and propagation [3,35,36]. Our current study further demonstrates that the microtubule depolymerizing reagent, nocodazole, or the expression of microtubule-destabilizing protein stathmin, significantly inhibits the enhancement of HIV-1 particle production by SOCS1, suggesting a possible role of the microtubule network in regular HIV-1 particle production.

Our previous report indicated that the targeted depletion of SOCS1 results in the prominent perinuclear accumulations of HIV-1 Gag in 293T cells [11]. Our current study shows that nocodazole treatment or stathmin expression only slightly affects Gag release in non-SOCS1 overexpressing cells. This difference might be attributable to the following two possibilities. First, SOCS1 may affect Gag at multiple points during trafficking and assembly, and a critical point could be prior to the microtubule-mediated events that can be affected by nocodazole or stathmin. Second, there are multiple pathways to the delivery of exogenously expressed Gag protein from the cytoplasm to the plasma membrane in addition to microtubule-directed transport. Furthermore, we are currently uncertain whether the Gag association with microtubules is mediated by other microtubule binding proteins in cooperation with SOCS1, or whether SOCS1 directly associates with HIV-1 Gag on the microtubules. Further careful analysis must be performed to elucidate these possibilities.

Acknowledgements

We thank Drs. A. Yoshimura, Y. Tanaka, K.P. Lu and J.A. Komano for providing materials, and R. Kimura, S. Takahama and H. Soeda for their excellent technical assistance. This work was supported in part by grants from the Ministry of Education, Culture, Sports, Science and Technology of Japan (20390136, 13226027, 14406009 and 1941075) and Human Health Science (H19-001) to N.Y. and A.R.

References

[1] Sorin, M. and Kalpana, G.V. (2006) Dynamics of virus–host interplay in HIV-1 replication. Curr. HIV Res. 4, 117–130.
[2] Trkola, A. (2004) HIV-host interactions: vital to the virus and key to its inhibition. Curr. Opin. Microbiol. 7, 407–411.
[3] Naghavi, M.H. and Goff, S.P. (2007) Retroviral proteins that interact with the host cell cytoskeleton. Curr. Opin. Immunol. 19, 402–407.
[4] Lama, J. and Planelles, V. (2007) Retrovirology 4, 52.
[5] Dong, X. et al. (2005) AP-3 directs the intracellular trafficking of HIV-1 Gag and plays a key role in particle assembly. Cell 120, 663–674.
[6] Perlman, M. and Resh, M.D. (2006) Identification of an intracellular trafficking and assembly pathway for HIV-1 gag. Traffic 7, 731–745.
[7] Alroy, I. et al. (2005) The trans-Golgi network-associated human ubiquitin-protein ligase POSH is essential for HIV type 1 production. Proc. Natl. Acad. Sci. USA 102, 1478–1483.
[8] Barr, S.D., Smiley, J.R. and Bushman, F.D. (2008) The interferon response inhibits HIV particle production by induction of TRIM22. PLoS Pathog. 4, e1000007.
[9] Joshi, A., Garg, H., Nagashima, K., Bonifacino, J.S. and Freed, E.O. (2008) GGA and Arf proteins modulate retrovirus assembly and release. Mol. Cell 30, 227–238.
[10] Ono, A., Ablan, S.D., Lockett, S.J., Nagashima, K. and Freed, E.O. (2004) Phosphatidylinositol (4, 5) bisphosphate regulates HIV-1 Gag targeting to the plasma membrane. Proc. Natl. Acad. Sci. USA 101, 14889–14894.
[11] Ryo, A. et al. (2008) SOCS1 is an inducible host factor during HIV-1 infection and regulates the intracellular trafficking and stability of HIV-1 Gag. Proc. Natl. Acad. Sci. USA 105, 294–299.
[12] Ryo, A. et al. (2003) Regulation of NF-kappaB signaling by Pin1-dependent prolyl isomerization and ubiquitin-mediated proteolysis of p65/RelA. Mol. Cell 12, 1413–1426.
[13] Wagner, R., Graf, M., Bieler, K., Wolf, H., Grunwald, T., Foley, P. and Uberla, K. (2000) Rev-independent expression of synthetic gag-pol genes of human immunodeficiency virus type 1 and simian immunodeficiency virus: implications for the safety of lentiviral vectors. Hum. Gene Ther. 11, 2403–2413.
[14] Stang, E., Blystad, F.D., Kazazic, M., Bertelsen, V., Brodahl, T., Raiborg, C., Stenmark, H. and Madshus, I.H. (2004) Cbl-dependent ubiquitination is required for progression of EGF receptors into clathrin-coated pits. Mol. Biol. Cell 15, 3591–3604.
[15] Sawasaki, T., Ogasawara, T., Morishita, R. and Endo, Y. (2002) A cell-free protein synthesis system for high-throughput proteomics. Proc. Natl. Acad. Sci. USA 99, 14652–14657.
[16] Vuong, B.Q. et al. (2004) SOCS-1 localizes to the microtubule organizing complex-associated 20S proteasome. Mol. Cell Biol. 24, 9092–9101.
[17] Westermann, S. and Weber, K. (2003) Post-translational modifications regulate microtubule function. Nat. Rev. Mol. Cell Biol. 4, 938–947.
[18] Kobayashi, T. and Yoshimura, A. (2005) Keeping DCs awake by putting SOCS1 to sleep. Trends Immunol. 26, 177–179.
[19] Kile, B.T., Schulman, B.A., Alexander, W.S., Nicola, N.A., Martin, H.M. and Hilton, D.J. (2002) The SOCS box: a tale of destruction and degradation. Trends Biochem. Sci. 27, 235–241.
[20] Jager, S., Gottwein, E. and Krausslich, H.G. (2007) Ubiquitination of human immunodeficiency virus type 1 Gag is highly dependent on Gag membrane association. J. Virol. 81, 9193–9201.
[21] Strack, B., Calistri, A., Accola, M.A., Palu, G. and Gottlinger, H.G. (2000) A role for ubiquitin ligase recruitment in retrovirus release. Proc. Natl. Acad. Sci. USA 97, 13063–13068.
[22] Naka, T. et al. (1997) Structure and function of a new STAT-induced STAT inhibitor. Nature 387, 924–929.
[23] Endo, T.A. et al. (1997) A new protein containing an SH2 domain that inhibits JAK kinases. Nature 387, 921–924.
[24] Starr, R. et al. (1997) A family of cytokine-inducible inhibitors of signalling. Nature 387, 917–921.
[25] Poole, E., Strappe, P., Mok, H.P., Hicks, R. and Lever, A.M. (2005) HIV-1 Gag-RNA interaction occurs at a perinuclear/centrosomal site; analysis by confocal microscopy and FRET. Traffic 6, 741–755.
[26] Greber, U.F. and Way, M. (2006) A superhighway to virus infection. Cell 124, 741–754.
[27] Benboudjema, L., Mulvey, M., Gao, Y., Pimplikar, S.W. and Mohr, I. (2003) Association of the herpes simplex virus type 1 Us11 gene product with the cellular kinesin light-chain-related protein PAT1 results in the redistribution of both polypeptides. J. Virol. 77, 9192–9203.
[28] Dohner, K. and Sodeik, B. (2005) The role of the cytoskeleton during viral infection. Curr. Top. Microbiol. Immunol. 285, 67–108.
[29] Jouvenet, N., Monaghan, P., Way, M. and Wileman, T. (2004) Transport of African swine fever virus from assembly sites to the plasma membrane is dependent on microtubules and conventional kinesin. J. Virol. 78, 7990–8001.
[30] Leblanc, J.J., Perez, O. and Hope, T.J. (2008) Probing the structural states of human immunodeficiency virus type 1 pr55gag by using monoclonal antibodies. J. Virol. 82, 2570–2574.
[31] Tang, Y., Winkler, U., Freed, E.O., Torrey, T.A., Kim, W., Li, H., Goff, S.P. and Morse 3rd, H.C. (1999) Cellular motor protein KIF-4 associates with retroviral Gag. J. Virol. 73, 10508–10513.
[32] Martinez, N.W., Xue, X., Berro, R.G., Kreitzer, G. and Resh, M.D. (2008) Kinesin KIF4 regulates intracellular trafficking and stability of the human immunodeficiency virus type 1 Gag polyprotein. J. Virol. 82, 9937–9950.
[33] Finzi, A., Orthwein, A., Mercier, J. and Cohen, E.A. (2007) Productive human immunodeficiency virus type 1 assembly takes place at the plasma membrane. J.Virol. 81, 7476–7490.
[34] Jouvenet, N., Neil, S.J., Bess, C., Johnson, M.C., Virgen, C.A., Simon, S.M. and Bieniasz, P.D. (2006) Plasma membrane is the site of productive HIV-1 particle assembly. PLoS Biol. 4, e435.
[35] Jolly, C., Mitar, I. and Sattentau, Q.J. (2007) Requirement for an intact T-cell actin and tubulin cytoskeleton for efficient assembly and spread of human immunodeficiency virus type 1. J. Virol. 81, 5547–5560.
[36] Handley, M.A., Paddock, S., Dall, A. and Panganiban, A.T. (2001) Association of Vpu-binding protein with microtubules and Vpu-dependent redistribution of HIV-1 Gag protein. Virology 291, 198–207.

 DOI 10.1002/eji.200939433 Eur. J. Immunol. 2009. 39: 2822–2830

European Journal of Immunology

Concurrent infection with *Heligmosomoides polygyrus* suppresses anti-*Plasmodium yoelii* protection partially by induction of $CD4^+CD25^+Foxp3^+$ Treg in mice

Kohhei Tetsutani[1], Kenji Ishiwata[2], Hidekazu Ishida[1], Liping Tu[1], Motomi Torii[3], Shinjiro Hamano[1,4], Kunisuke Himeno[1] and Hajime Hisaeda[1]

[1] Department of Parasitology, Kyushu University Graduate School of Medical Science, Fukuoka, Japan
[2] Department of Tropical Medicine, The Jikei University School of Medicine, Tokyo, Japan
[3] Department of Molecular Parasitology, Ehime University School of Medicine, Ehime, Japan
[4] Department of Parasitology, Institute of Tropical Medicine (NEKKEN) and the Global COE program, Nagasaki University, Nagasaki, Japan

Malaria and intestinal nematode infection are widespread and co-infection frequently occurs. We investigated whether co-infected intestinal nematodes modulate immunity against co-existing malaria parasites. Infection of C57BL/6 mice with *Plasmodium yoelii* 17XNL (Py) was transient and self-limiting, but preceding infection with *Heligmosomoides polygyrus* (Hp), a mouse intestinal nematode, exacerbated malaria resulting in higher parasite burdens and poor survival of the mice. Co-infection with Hp led to reduced Py-responsive proliferation and IFN-γ production of spleen cells, and higher activation of $CD4^+CD25^+Foxp3^+$ Treg. *In vivo* depletion of Treg recovered anti-Py immunity and rescued co-infected mice from exacerbated malaria. However, we did not observe any obvious *ex vivo* activation of Treg by either Hp products or living worms. Our results suggest that intestinal nematodes moderate host immune responses during acute malaria infection by aggressive activation of Treg. Elucidation of the mechanisms of Treg activation *in situ* is a target for future analyses.

Key words: Adaptive immunity · Malaria · Intestinal nematode · Regulatory T cell

Introduction

Malaria is the most widespread and deadliest parasitic disease, and it causes hundreds of millions of clinical cases and millions of deaths annually worldwide. The severity of the disease is strongly related to the malaria parasite species, parasite density and immune responses of the host. Protective immunity against malaria develops very slowly, and individuals living in endemic areas suffer from repeated infections. The major reason why immunity to malaria is difficult to develop is that malaria parasites effectively evade host immunity in several ways. Antigenic diversity/variation allows parasites to escape immune recognition [1, 2]. They also actively suppress immunity *via* induction of Treg [3, 4], effector T-cell apoptosis [5] or dysfunctions of APCs [6]. These immune evasion mechanisms also make it difficult to develop effective vaccines against malaria.

Environmental factors, such as exposure to infective vectors [7], nutritional status [8], medical/public health interventions [9] and concurrent infections with other pathogens [10], also affect the outcome of the disease. Among infections, chronic but mostly asymptomatic infection with intestinal helminths is the most

Correspondence: Dr. Kohhei Tetsutani
e-mail: tetztani@gmail.com

prevalent in malarial areas [11, 12] (http://gamapserver.who.int/mapLibrary/Files/Maps/global_cases.jpg, http://www.who.int/intestinal_worms/epidemiology/map/en/index.html) and the population in a given area tends to suffer from both infections. Generally, as well as schistosomes [13] or filarias [14], intestinal helminths are known to modulate, and mainly suppress, host immune responses [15]. Indeed, studies in Thailand showed that infection with intestinal helminths increased the frequency of malaria episodes, but decreased malaria-associated serious inflammations, such as cerebral malaria, acute renal failure or pulmonary edema [16, 17]. These observations suggest that intestinal helminths suppress host responses of both protective immunity and inflammation during malaria infection. Therefore, it is important to understand the relationship between co-infection and host immune responses for effective control of malaria.

Several researchers have studied the effects of co-infection with intestinal helminths on the course of malaria using mouse models and reported that co-infection causes rapid growth of malaria parasites *in vivo* [18–20]. A good experimental model is the mouse intestinal nematode *Heligmosomoides polygyrus* (Hp), which resides in the upper small intestine for a long time and is known to modulate host responses through various mechanisms [21, 22]. Su *et al.* [18] described that proliferation of immune cells in response to the malaria Ag or production of anti-malaria Ab was suppressed with the induction of regulatory cytokines during co-infection with Hp and *Plasmodium chabaudi*. Unlike the results from human studies in Thailand, Hp did not attenuate inflammation-associated experimental cerebral malaria, but it did suppress anti-parasite immunity during infection with *P. berghei* ANKA [20]. These observations are compatible with our findings from studies on mice infected with Hp [21]. However, the interactions between nematodes inside the intestine and immune systems are still not well understood.

Here, we examined the effects of co-infection with Hp on the course of infection with the rodent malaria parasite *P. yoelii* 17XNL (Py) by focusing on $CD4^+CD25^+Foxp3^+$ Treg as key factors linking nematodes and suppressed host protection. We found that Hp and Py co-infection induced strongly activated Treg, which suppressed anti-Py effector mechanisms, increased malaria parasite growth *in vivo* and deteriorated survival of mice.

Results

Preceding infection with Hp deteriorates Py infection

First, we infected Hp-harboring mice with the non-lethal malaria strain Py. As previously reported [4], infection with Py alone exhibited transient elevation of parasitemia and a spontaneous cure within 3–4 wk (Fig. 1A). Co-infection with Hp caused rapid growth of Py at the early and late phases of infection (Fig. 1A), and all the mice died (Fig. 1B). Unlike the rodent parasite *P. berghei*, Py is widely considered not to induce fatal host-damaging inflammations, such as liver injury [23]. Therefore, the cause of death of the co-infected mice was supposed to be failure to eradicate the parasites, suggesting that the presence of Hp suppressed host immune responses against Py.

Co-infection with Hp suppresses adaptive immune responses against Py

Next, we analyzed the immune responses to Py in Hp-harboring mice after infection with Py. Splenocytes isolated from co-infected mice were stimulated with Py-parasitized RBC (pRBC) and analyzed for their proliferative responses (Fig. 2A). Whole spleen cells from mice infected with Py alone showed remarkable proliferation in response to pRBC. However, preceding infection with Hp significantly suppressed this proliferation. Similar results were obtained when $CD4^+CD25^-$ spleen cells were examined. The suppression was not specific for Py Ag because responses to ConA were also suppressed. We also analyzed production of IFN-γ, one of the indispensable effector molecules against malaria parasites [24]. Consistent with the proliferative responses, production of IFN-γ by spleen cells of mice infected

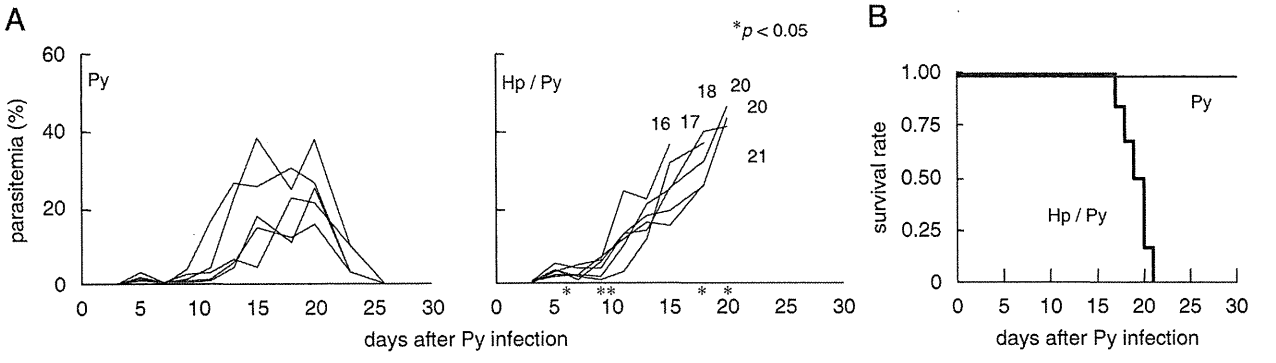

Figure 1. *H. polygyrus* and *P. yoelii* NL co-infection in C57BL/6N male mice. Mice ($n = 5–7$) were infected with Hp larvae orally and then i.p. infected with Py pRBC (2.5×10^4 cells/mouse) 2 wk later. Parasitemia (A) and survival (B) of the mice were monitored daily. Each line shows the parasitemia curve of an individual mouse, and the numbers show the death day of each individual (A). Parasitemia was analyzed statistically by Student's t-test. Asterisks show significant differences at the indicated *p* value. The experiment was repeated three times with similar results.

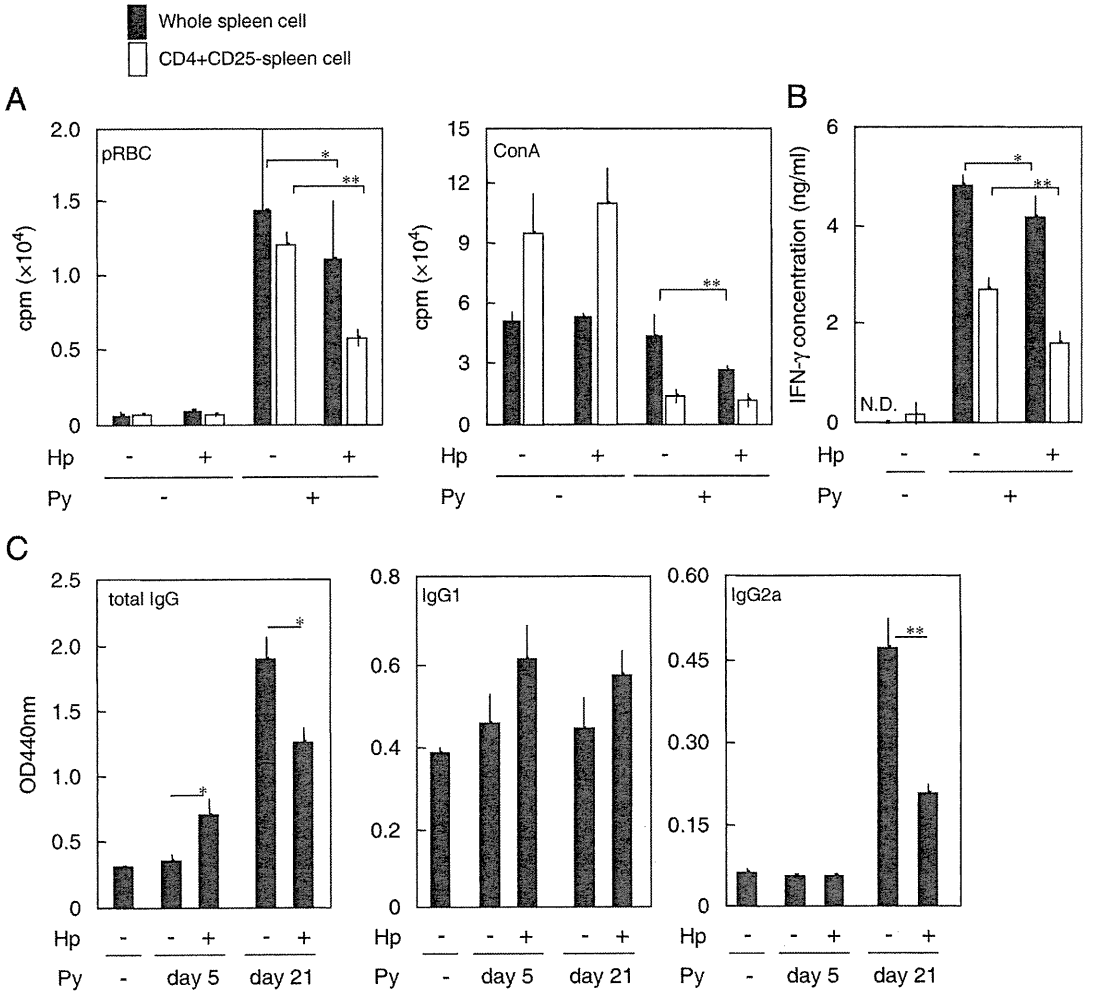

Figure 2. Effects of co-infection with Hp on immune responses against Py. Spleen cells or $CD4^+CD25^-$ spleen cells were isolated from mice co-infected with Hp and Py at 5 days after Py infection. Whole spleen cells (2×10^5; closed bars) or $CD4^+CD25^-$ cells (1×10^5) and $CD11c^+$ cells (1×10^4) from uninfected mice (open bars) were cultured with pRBC (2×10^5) or ConA (2.5 μg/mL). (A) Proliferation was analyzed by ^{3}H-thymidine uptake. (B) IFN-γ concentrations in the culture supernatants with pRBC were measured by ELISA. (C) Anti-Py IgG, IgG1 or IgG2a Ab in sera taken at the indicated days after Py infection were measured by ELISA using Py Ag. (D) $CD11c^+$ cells (1×10^4) were isolated from mice co-infected with Hp and Py at 5 days after Py infection and cultured with $CD4^+CD25^-$ cells (1×10^5) from Py-infected mice and pRBC (2×10^5). Proliferation was analyzed by ^{3}H-thymidine uptake. Data represent the means ±SE of triplicate samples in a representative of 3–6 repeated experiments. $^*p<0.05$, $^{**}p<0.01$; between the samples linked with horizontal lines, Student's *t*-test.

with Py was significantly suppressed by preceding infection with Hp (Fig. 2B). These results clearly indicate that co-infection with Hp suppresses cellular immune responses. Humoral immunity, represented by IgG specific for malaria parasites, was subsequently analyzed (Fig. 2C). Infection with Py alone led to the development of IgG2a-dominant Ab responses at 21 days after infection, but had no effect at 5 days after infection. Despite the higher parasitemia at the early phase, co-infection with Hp rather enhanced the production of IgG1. Conversely, it remarkably reduced the production of IgG2a in curable mice singly infected with Py, suggesting that the Ab responsible for protection at the late phase may be IgG2a. These results demonstrate that the increased Py parasitemia at the early stage of infection is due to suppression of cellular responses, rather than Ab responses. Therefore, we subsequently focused on the suppression of cellular responses at the early phase.

Co-infection with Hp and Py induces aggressively suppressive Treg

In a previous report, we demonstrated that activation of Treg occurs during infection with a lethal strain of *P. yoelii* [4]. In addition, it has been reported that the functions of Treg are altered in mice infected with Hp [25]. These observations led us to analyze the Treg behaviors in co-infected mice. As early as 5 days after infection with Py, the proportion of $CD4^+CD25^+$ $Foxp3^+$ cells was increased in the spleen, as well as MFI of either

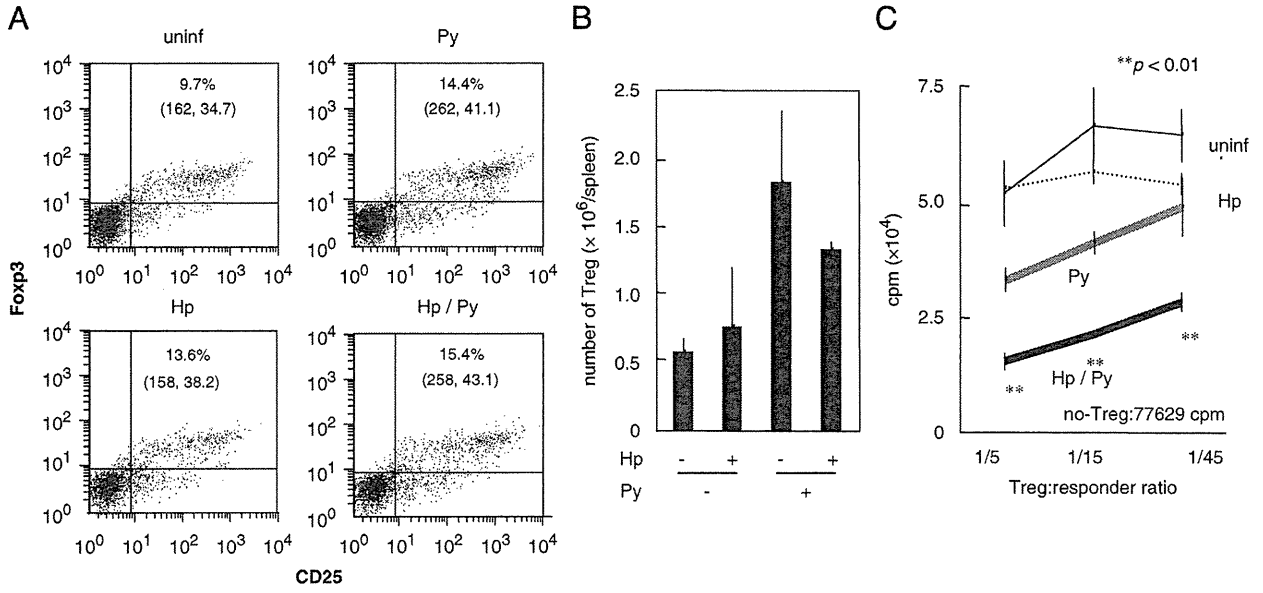

Figure 3. $CD4^+CD25^+Foxp3^+$ cells in Hp+Py co-infection. Spleen cells stained with fluorochrome-conjugated anti-CD4, anti-CD25 and anti-Foxp3 Ab were analyzed by flow cytometry at 5 days after infection with Py. (A) The dot plots represent the expression levels of CD25 and Foxp3 in CD4-gated cells from the indicated mice. Percentage inside of each plot shows the frequency of $CD4^+CD25^+Foxp3^+$ cells in total $CD4^+$ cells. The number inside of brackets shows the mean fluorescent intensity of CD25 (left) and Foxp3 (right). (B) The $CD4^+CD25^+Foxp3^+$ cell populations in individual spleens were calculated. (C) The suppressive functions of Treg from co-infected mice were analyzed at 5 days after infection with Py. Splenic Treg from the indicated mice were cultured with $CD4^+CD25^-$ cells (1×10^5) as responders and $CD11c^+$ cells (1×10^4) obtained from the spleens of uninfected mice in the presence of ConA (2.5 μg/mL) at the indicated frequencies. The proliferation of responders was analyzed by ^3H-thymidine uptake. Data are presented as the means ±SE of three samples in a representative of three repeated experiments. Asterisks show significant differences by Student's t-test between Treg from Py-infected and Hp+Py-infected mice at the indicated p value.

CD25 or Foxp3 (Fig. 3A). The absolute number of $CD4^+CD25^+$ $Foxp3^+$ cells in individual spleens, calculated from the cell frequency by flow cytometry, was also increased (Fig. 3B). The amount of Foxp3 expressed in Treg may influence their functions [26], suggesting that Treg with the higher Foxp3 MFI observed in co-infection may have enhanced suppressive function. Thus, the suppressive function of Treg was determined by analyzing the degree of suppression of TCR-triggered T-cell proliferation at this time point. Co-infection with Hp enhanced the suppressive activity of Treg, but did not affect the number of Treg (Fig. 3B, C). These results suggest that co-infection with Hp and Py induces Treg more aggressively than single infection with Py, resulting in deteriorated malaria infection associated with suppressed cellular responses against Py.

In vivo depletion of Treg partially abolishes the suppressed protection against Py

To confirm that induction of Treg in mice co-infected with Hp and Py is responsible for the deteriorated infection with Py, we depleted Treg by i.p. application of an anti-CD25 Ab. This treatment depleted 85% of the $CD4^+CD25^+Foxp3^+$ Treg in the spleen, as evaluated by Foxp3 intracellular flow cytometry, at 5 days after infection (Fig. 4A). However, the depletion effect was transient and Treg were detected in mice treated with the anti-CD25 Ab at similarly high levels to those in control mice at 2 wk after the treatment (data not shown). As previously shown, infection with Py was self-limiting, and again mice co-infected with Hp suffered from higher parasitemia and finally succumbed to infection with Py (Fig. 4B, C). Depletion of Treg significantly decreased the parasitemia at the early phase of infection in co-infected mice. Furthermore, 40% of the co-infected mice depleted of Treg were able to limit the parasitemia and they survived (Fig. 4B, C).

The anti-malarial effector mechanisms were altered by depletion of Treg. The suppression of IFN-γ production by splenic $CD4^+$ T cells in response to pRBC observed in co-infected mice was clearly reversed after removal of Treg (Fig. 4D). Alterations in Ab responses due to co-infection with Hp, namely suppression of IgG and IgG2a at the later phase and enhancement of IgG at the early phase, were all offset by the removal of Treg (Fig. 4E). These results suggest that the deteriorated malaria infection in mice co-infected with Hp and Py was partially due to aggressive activation of Treg.

Hp worm products and living worms do not directly activate Treg *in vitro*

The preceding existence of Hp activates Treg in terms of enhanced suppressive functions during infection with Py. To investigate how co-infection with Hp induces stronger Treg, we performed *in vitro* Treg activation assays using various Hp products. Splenic Treg from Py-infected mice were stimulated

